

Penultimate modeling of spatial extremes: statistical inference for max-infinitely divisible processes

Raphaël Huser¹, Thomas Opitz² and Emeric Thibaud³

December 14, 2024

Abstract

Extreme-value theory for stochastic processes has motivated the statistical use of max-stable models for spatial extremes. However, fitting such asymptotic models to maxima observed over finite blocks is problematic when the asymptotic stability of the dependence does not prevail in finite samples. This issue is particularly serious when data are asymptotically independent, such that the dependence strength weakens and eventually vanishes as events become more extreme. We here aim to provide flexible sub-asymptotic models for spatially indexed block maxima, which more realistically account for discrepancies between data and asymptotic theory. We develop models pertaining to the wider class of max-infinitely divisible processes, extending the class of max-stable processes while retaining dependence properties that are natural for maxima: max-id models are positively associated, and they yield a self-consistent family of models for block maxima defined over any time unit. We propose two parametric construction principles for max-id models, emphasizing a point process-based generalized spectral representation, that allows for asymptotic independence while keeping the max-stable extremal- t model as a special case. Parameter estimation is efficiently performed by pairwise likelihood, and we illustrate our new modeling framework with an application to Dutch wind gust maxima calculated over different time units.

Keywords: asymptotic dependence and independence; block maximum; extreme event; max-infinitely divisible process; sub-asymptotic modeling.

¹Computer, Electrical and Mathematical Sciences and Engineering (CEMSE) Division, King Abdullah University of Science and Technology (KAUST), Thuwal 23955-6900, Saudi Arabia. E-mail: raphael.huser@kaust.edu.sa

²INRA, UR546 Biostatistics and Spatial Processes, 228, Route de l'Aérodrome, CS 40509, 84914 Avignon, France. E-mail: thomas.opitz@inra.fr

³Ecole Polytechnique Fédérale de Lausanne, EPFL-FSB-MATHAA-STAT, Station 8, 1015 Lausanne, Switzerland. E-mail: emeric.thibaud@epfl.ch

1 Introduction

Max-stable processes have emerged as useful models for the statistical analysis and prediction of extreme events in the context of spatially indexed observations; see [Davison et al. \(2012\)](#) and [Davison and Huser \(2015\)](#) for recent reviews, and [Westra and Sisson \(2011\)](#), [Davison and Gholamrezaee \(2012\)](#) and [Stephenson et al. \(2016\)](#) for environmental applications. Dependence at extreme levels must be properly captured to accurately estimate probabilities of extreme events and their spatial extent, and to quantify the uncertainty. Max-stable processes are usually fitted based on observed spatial block-wise maxima with blocks taken to match natural cycles such as months or years for instance. Since block maxima are stochastically increasing as a function of the block size, calculating them over larger blocks provides a better representation of the data's tail properties. The motivation underlying the use of max-stable processes stems from asymptotic theory, and assumes that maxima over large blocks of finite size are already sufficiently close to their asymptotic regime. However, empirical studies on environmental spatial extremes have revealed that this assumption is not always satisfied; often, weakening of spatial dependence is observed as events become more extreme ([Huser et al., 2017](#); [Huser and Wadsworth, 2017](#)). This suggests that classical asymptotic models may not be appropriate at observable sub-asymptotic levels, and extrapolation to yet-unobserved extreme levels based on limit max-stable models might be dubious.

To illustrate the limitations of max-stable models, we compute empirical extremal coefficients, a measure of extremal dependence for max-stable models, estimated for the Dutch wind speed dataset analyzed in Section 5. With unit Fréchet margins, the joint distribution of a max-stable process $Z(\mathbf{s})$ observed at D sites $\mathbf{s}_1, \dots, \mathbf{s}_D \in \mathcal{S} \subset \mathbb{R}^d$, may be written as $\Pr\{Z(\mathbf{s}_1) \leq z_1, \dots, Z(\mathbf{s}_D) \leq z_D\} = \exp\{-V(z_1, \dots, z_D)\}$, where V denotes the exponent function. The multivariate extremal coefficient, defined in (6) as $\theta_D(z) = zV(z, \dots, z) \in [1, D]$, reflects the equivalent number of independent variables at level z , and by max-stability $\theta_D(z) \equiv \theta_D$ is constant with z . Figure 1 displays empirical extremal coefficients $\hat{\theta}_D^{emp}(z) = -z \log\{n^{-1} \sum_{i=1}^n I(z_{i1} \leq z, \dots, z_{iD} \leq z)\}$, where z_{ij} denotes the i th daily, weekly and monthly wind speed maximum observed at the j th Dutch monitoring station (for $D = 30$ stations), plotted as a function of level z . This reveals that $\theta_D(z)$ is increasing rather than being constant with respect to z and the time unit over which maxima are calculated, which contradicts max-stability and suggests a weakening of the spatial dependence as extreme wind speeds over the Netherlands become stronger. More

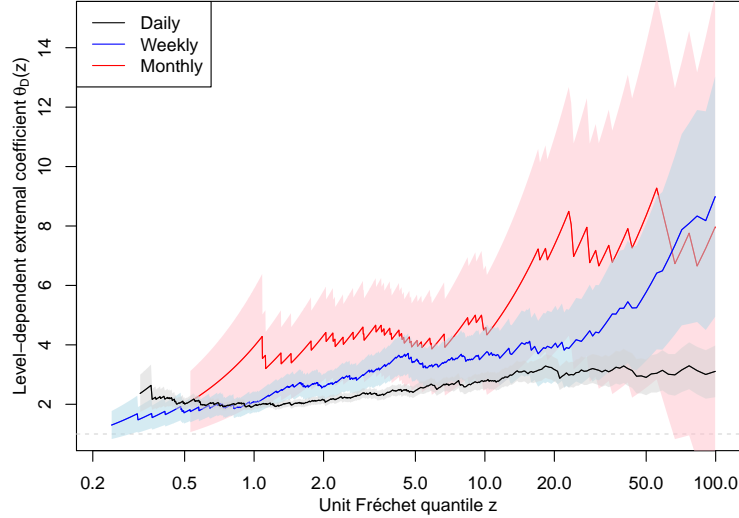


Figure 1: Empirical extremal coefficients $\hat{\theta}_D^{emp}(z)$ (solid curves) for the Dutch wind speed data analyzed in Section 5, plotted as a function of unit Fréchet quantile z (on a log scale), based on daily (black), weekly (blue) and monthly (red) maxima. Shaded areas represent 95%-confidence intervals based on the delta method, ignoring weak temporal dependence.

flexible dependence structures capturing this feature might perform better, as confirmed in Section 5. Nonparametric copula-based hypothesis tests of max-stability have been developed (Kojadinovic *et al.*, 2011), but we expect them to have only weak power in the spatial context with many variables and relatively few temporal replicates.

John W. Tukey stated in a 1961 Princeton University technical report (Tukey, 1961) that “the purpose of asymptotic theory in statistics is simple: to provide usable approximations before passage to the limit”. Following this wise guideline, we propose in this paper new penultimate models for capturing dependence in (finite) block maxima, that are flexible generalizations of ultimate max-stable models but still possess attractive theoretical properties reflecting the particular structure of maxima. In the univariate context, penultimate approximations for the generalized extreme-value (GEV) distribution have been studied by Kaufmann (2000), and similar ideas have been exploited for modeling sub-asymptotic threshold exceedances by Papastathopoulos and Tawn (2013). Penultimate models of extremal dependence have been proposed by Bortot and Tawn (1998) in the time series context and by Wadsworth and Tawn (2012) and Huser *et al.* (2017) in the spatial context based on threshold exceedances. Max-infinitely divisible (max-id) processes are natural models for penultimate maxima data since they accommodate the specific type of positive dependence resulting from the operation of taking pointwise maxima of independent and identically dis-

tributed (iid) processes. They extend the class of max-stable processes while relaxing their restrictive stability properties. Max-id models ensure validity of distributions of extremes and derived quantities after a change of temporal support, e.g., when characterizing the joint tail of daily iid variables based on a distribution fitted to yearly maxima.

A major contribution of this paper is to propose general construction principles for building new parametric max-id models, and we characterize their dependence properties, providing more flexible alternatives to max-stable models at sub-asymptotic regimes. We design max-id models for spatial maxima that bridge asymptotic independence and dependence by exploiting recent results on Gaussian scale mixtures used for high threshold exceedances ([Huser et al., 2017](#)). The max-stable submodel in this parametric family is the widely-used extremal- t process ([Opitz, 2013](#)). Increased tail flexibility of our new models makes them attractive for modeling maxima taken over relatively small blocks such as days or weeks, which also increases the effective sample size, leading to improved statistical efficiency.

In the literature, there are only few applications of max-id models beyond max-stability, but theoretical properties have been explored in several papers ([Giné et al., 1990](#); [Dombry and Eyi-Minko, 2013](#)). One exception includes [Padoan \(2013\)](#), who proposed a specific Gaussian-based max-id model whose dependence strength varies with the intensity of the extreme event. Our modeling approach differs fundamentally by extending the spectral representation of max-stable processes. Moreover, we exploit many developments made for max-stable processes, including pairwise likelihood inference and simulation methods, and we explore how to adapt them to the max-id context.

As monotone increasing marginal transformations do not affect the max-id structure, we propose to use the (max-stable) generalized extreme value (GEV) limit distribution for modeling margins; this three-parameter distribution has been used extensively for modeling univariate maxima and is usually flexible enough. Therefore, our approach boils down to using a max-id dependence structure (i.e., max-id copula) with GEV margins.

In Section 2, we recall theoretical results and properties of max-id and max-stable distributions. In Section 3, we discuss two general construction principles for max-id processes, focusing on a spectral construction. We then propose models capturing both asymptotic dependence and independence. Likelihood-based inference is discussed in Section 4, and an application to wind gusts is presented in Section 5. Section 6 concludes with some discussion.

2 Max-infinitely divisible distributions

2.1 Definition and Poisson process construction

When a random vector \mathbf{Y} has joint distribution F , then the componentwise maximum vector of m iid copies of \mathbf{Y} has distribution F^m . This implies that for any distribution F and any integer $m \in \mathbb{N}$, F^m is always a valid distribution. A max-infinitely divisible (or max-id in short) distribution guarantees the opposite statement: a distribution function G on \mathbb{R}^D is max-id if $G^{1/m}$ defines a valid distribution for any integer $m \in \mathbb{N}$. Hence, a max-id distribution G arises as the distribution of the componentwise maximum of m iid random variables with distribution $F = G^{1/m}$, for any $m \in \mathbb{N}$. By considering F^m with $m = p/q$, $p, q \in \mathbb{N}$, combined with a continuity argument, this extends to any real number $r > 0$: a distribution G is max-id if and only if G^r is a valid distribution for any $r > 0$. In practice, this property permits to switch from the joint distribution G of the componentwise maximum over a given time unit to alternative time units and in particular to the distribution F of the original events. For example, by fitting a max-id model to annual maxima of a variable of interest, conclusions may be drawn for weekly, daily, or even subdaily maxima of the same variable, modulo non-stationary and temporal dependence aspects. Unlike the univariate case, multivariate distributions are not always max-id. A simple counter-example is the bivariate standard Gaussian distribution $\Phi_2(\cdot; \rho)$ with negative correlation ρ (Resnick, 1987, Section 5.2). Figure 2 displays the “density” $\frac{\partial^2}{\partial z_1 \partial z_2} \Phi_2^{1/m}(z_1, z_2; \rho)$ with $\rho = -0.5$ and $m = 2, 10$. Such a function would always be positive for any value of $m > 1$ if $\Phi_2(\cdot; -0.5)$ were max-id, but Figure 2 reveals large areas with negative values, especially for large m .

To propose useful spatial models of max-id processes, we will exploit a constructive characterization of max-id distributions based on a Poisson process representation (Resnick, 1987, Chapter 5). For simplicity, we provide the following definitions and characterizations in terms of multivariate distributions. The generalization to stochastic processes over continuous space is straightforward, albeit requiring some heavier notation and the choice of appropriate function spaces (Giné et al., 1990). In the following, we identify the Euclidean space \mathbb{R}^D with its extension to infinity values $[-\infty, \infty]^D$.

We consider a Poisson point process defined on the domain $E = [\ell_1, \infty] \times \dots \times [\ell_D, \infty] \subseteq \mathbb{R}^D$ with mean measure $\Lambda \geq 0$, where the lower endpoint $\boldsymbol{\ell} = (\ell_1, \dots, \ell_D)^T \in [-\infty, \infty)^D$ may contain components that are equal to $-\infty$. For theoretical reasons, we further impose that Λ must be a Radon measure on $E \setminus \{\boldsymbol{\ell}\}$ such that Borel sets A with infinite mass $\Lambda(A)$ may

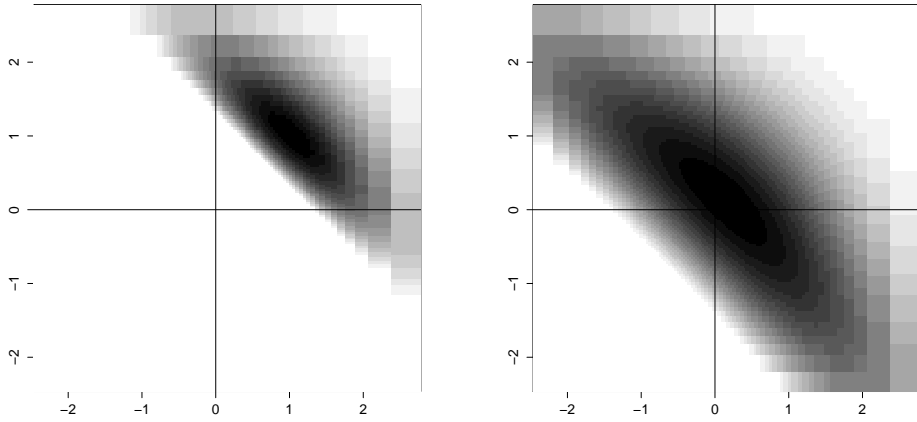


Figure 2: Function $\frac{\partial^2}{\partial z_1 \partial z_2} \Phi_2^{1/m}(z_1, z_2; \rho)$ for a bivariate standard Gaussian distribution Φ_2 with correlation coefficient $\rho = -0.5$, for $m = 2$ (left) and $m = 10$ (right). The grey region corresponds to negative values, with darker areas indicate higher absolute values.

only arise when the closure of A contains the lower endpoint $\boldsymbol{\ell}$. Extending the measure Λ to \mathbb{R}^D by setting $\Lambda(A) = \Lambda(A \cap E)$, we construct a Poisson point process on $E \setminus \{\boldsymbol{\ell}\}$ as

$$\{\mathbf{X}_i, i = 1, \dots, N\} \sim \text{PPP}(\Lambda), \quad N \in \mathbb{N}_0 \cup \{\infty\}. \quad (1)$$

We then define a random vector $\mathbf{Z} \in \mathbb{R}^D$ with support contained in E as the componentwise maximum over the points \mathbf{X}_i and the lower endpoint $\boldsymbol{\ell}$, i.e.,

$$\mathbf{Z} := \max \left(\max_{i=1,2,\dots} \mathbf{X}_i, \boldsymbol{\ell} \right). \quad (2)$$

The value $\mathbf{Z} = \boldsymbol{\ell}$ arises when the Poisson process contains no points in $E \setminus \{\boldsymbol{\ell}\}$. From [Resnick \(1987, Proposition 5.8\)](#), it follows that \mathbf{Z} is max-id, and its joint distribution function is

$$G(\mathbf{z}) = \exp \left(-\Lambda [-\infty, \mathbf{z}]^C \right), \quad \mathbf{z} \in E, \quad G(\mathbf{z}) = 0, \quad \mathbf{z} \in E^C, \quad (3)$$

with A^C denoting the complement of the set A . Result (3) can be easily derived by noticing that the event $\{\mathbf{Z} \leq \mathbf{z}\}$, $\mathbf{z} \in E$, is equivalent to having no points \mathbf{X}_i in $[-\infty, \mathbf{z}]^C$. The measure Λ is called the exponent measure of G , and $V(\mathbf{z}) = \Lambda [-\infty, \mathbf{z}]^C$ is called exponent function. To ensure that \mathbf{Z} has no components with value $+\infty$, we further impose the theoretical restriction $\Lambda \{ \mathbf{z} : \max_{j=1,\dots,D} z_j = \infty \} = 0$. The Poisson process representation based on (1) and (2) is helpful for intuitive interpretation (§3.3.1), modeling (§3.2, §3.3.1 and §3.3.2) and simulation (§3.3.3).

Any univariate distribution function is max-id. If a random vector $\mathbf{Z} = (Z_1, \dots, Z_D)^T$ is max-id, the marginally transformed vector $\{h_1(Z_1), \dots, h_D(Z_D)\}^T$ with nondecreasing functions h_j , $j = 1, \dots, D$ remains max-id. Therefore, the max-id property concerns primarily

the dependence structure (i.e., the copula) and not the margins. Any random vector \mathbf{Z} with independent components Z_j is max-id with exponent measure concentrated on the half-axes $\{\ell_1\} \times \dots \times \{\ell_{j-1}\} \times [\ell_j, \infty] \times \{\ell_{j+1}\} \times \dots \times \{\ell_D\}$, $j = 1, \dots, D$, and any fully dependent random vector is also max-id.

2.2 Dependence properties

Max-id random vectors \mathbf{Z} are associated (Resnick, 1987, Proposition 5.29), meaning that for any choice of nondecreasing functions $h_i : \mathbb{R}^D \rightarrow \mathbb{R}$ such that $h_i(\mathbf{Z})$ has finite second moments, $i = 1, 2$, one has $\text{cov}\{h_1(\mathbf{Z}), h_2(\mathbf{Z})\} \geq 0$ (Esary et al., 1967). In other words, a certain form of positive dependence prevails; see also Alzaid and Proschan (1994). This shows that any random vector with negative correlation between some of its components cannot be max-id.

The tail dependence of a max-id distribution is closely related to the tail behavior of the exponent measure Λ . By applying the first-order Taylor expansion $\exp(-x) \sim 1 - x$ for small $x \approx 0$, we get from (3) that

$$1 - G(\mathbf{z}) = 1 - \exp\left(-\Lambda[-\infty, \mathbf{z}]^C\right) \sim \Lambda[-\infty, \mathbf{z}]^C, \quad \min_{j=1, \dots, D} z_j \rightarrow \infty. \quad (4)$$

More generally, whenever an event A is “extreme” in the sense that $A \subseteq [-\infty, \mathbf{z}]^C$ for a vector \mathbf{z} with all of its components being large, one can use (4) to approximate tail probabilities as $\Pr(\mathbf{Z} \in A) \approx \Lambda(A)$.

If a max-id distribution G with exponent measure Λ is used to model the componentwise maximum over m iid random vectors with distribution F such that $F^m = G$, then

$$F(\mathbf{z}) = G^{1/m}(\mathbf{z}) = \exp\left(-\Lambda[-\infty, \mathbf{z}]^C / m\right), \quad (5)$$

which gives the first-order tail approximation $1 - F(\mathbf{z}) \approx \Lambda[-\infty, \mathbf{z}]^C / m$ when $\mathbf{z} \gg \boldsymbol{\ell}$. Knowledge of the tail properties of Λ is paramount to understanding the tail characteristics of F . When Λ has finite mass, then $F(\boldsymbol{\ell}) = \exp\{-\Lambda(\boldsymbol{\ell})/m\}$, and with increasing m more and more mass concentrates on $\boldsymbol{\ell}$; such behavior does not arise when Λ has infinite mass. Consequences of this for modeling are further discussed in §3.1.

There is no loss of generality in assuming that the distribution G in (3) has common margins, because the max-id property concerns the dependence structure. In the extreme-value literature, it is common to assume unit Fréchet margins, in which case $\boldsymbol{\ell} = \mathbf{0}$, $E =$

$[\mathbf{0}, \infty]$ and $\Lambda(\{\mathbf{z} : z_j > z\}) = 1/z$ such that the max-id vector $\mathbf{Z} = (Z_1, \dots, Z_D)^T$ satisfies $\Pr(Z_j \leq z) = \exp(-1/z)$, $z > 0$, $j = 1, \dots, D$. Such a random vector is called simple max-id. A useful summary of the dependence strength for simple max-id distributions is the level-dependent extremal coefficient (Padoan, 2013), defined at quantile level $z > 0$, by

$$\theta_D(z) = zV(\mathbf{z}) = z\Lambda[-\infty, \mathbf{z}]^C \in [1, D], \quad \mathbf{z} = (z, \dots, z)^T \in \mathbb{R}^D. \quad (6)$$

From this definition and from (3), it follows that

$$\Pr(Z_1 \leq z, \dots, Z_D \leq z) = \exp\{-V(z, \dots, z)\} = \exp(-1/z)^{\theta_D(z)}, \quad (7)$$

so the extremal coefficient can be interpreted, at the level z , as the equivalent number of independent variables amongst Z_1, \dots, Z_D , interpolating between perfect dependence when $\theta_D(z) = 1$ and independence when $\theta_D(z) = D$. In the bivariate case, we have that

$$\chi(z) = \Pr(Z_1 > z \mid Z_2 > z) = \frac{1 - 2 \exp(-1/z) + G(z, z)}{1 - \exp(-1/z)} \sim 2 - zV(z, z) = 2 - \theta_2(z), \quad (8)$$

as $z \rightarrow \infty$. When $\chi = \lim_{z \rightarrow \infty} \chi(z) = 0$, which occurs when $\theta_2(z) \rightarrow 2$ or more strongly when $\theta_D(z) \rightarrow D$, as $z \rightarrow \infty$, the pair of variables $(Z_1, Z_2)^T$ is called asymptotically independent, whilst they are asymptotically dependent if $\chi > 0$. Asymptotic independence reflects scenarios of weakening and ultimately vanishing dependence strength as a function of the quantile level z . Notice that the expansion (8) remains valid when the distribution G is replaced by $F = G^{1/m}$ in (5), for any m . Hence, $\theta_2(z)$, or equivalently $\chi(z)$, determines the tail behavior on the scale of the observations or maxima.

2.3 Max-stable distributions

Max-stable processes have been widely used for modeling spatial extremes (Davison et al., 2012) in virtue of their central role as the only possible non-degenerate limit distributions of renormalized componentwise maxima. If a distribution F is such that for some sequences of vectors $\mathbf{a}_m > \mathbf{0}$ and \mathbf{b}_m ,

$$F^m(\mathbf{a}_m \mathbf{z} + \mathbf{b}_m) \rightarrow G(\mathbf{z}), \quad m \rightarrow \infty, \quad (9)$$

where the distribution G has non-degenerate margins, then the limit G is max-stable. It follows that G satisfies, for any integer $m \in \mathbb{N}$ (and by extension for any real $r > 0$), the stability property $G^{1/m}(\mathbf{z}) = G(\boldsymbol{\alpha}_m \mathbf{z} + \boldsymbol{\beta}_m)$ with multivariate normalizing vectors $\boldsymbol{\alpha}_m > \mathbf{0}$ and $\boldsymbol{\beta}_m$.

Max-stable processes form a smaller subclass within the class of max-id distributions. Max-stability implies that the distributions of a random vector and of its componentwise maxima belong to the same location-scale family, and in particular that the dependence structure (i.e., the copula) is invariant. If G is max-stable with unit Fréchet marginal distributions (i.e., G is simple max-stable), then $E = [\mathbf{0}, \infty]$, $\Lambda(\{\mathbf{z} : z_j > z\}) = 1/z$, and $t\Lambda(tA) = \Lambda(A)$ for all $t > 0$. In particular, this last property states that the exponent measure Λ and the exponent function $V(\mathbf{z}) = \Lambda[-\infty, \mathbf{z}]^C$ of a max-stable vector are both homogeneous of order -1 , implying that the extremal coefficient $\theta_D(z) \equiv \theta_D$ defined in (6) is constant with level $z > 0$. However, this rigid stability assumption implies that max-stable models can only capture asymptotic dependence or exact independence, but fail at representing weakening dependence; recall (8). This is often too strong an assumption for environmental data (recall Figure 1), due to the convergence in (9) having manifestly not taken place for finite block sizes m . The broader class of max-id models allows to gain in flexibility by getting rid of this stability requirement. By analogy with (2), simple max-stable processes are often defined constructively through their spectral representation (de Haan, 1984; Schlather, 2002)

$$Z(\mathbf{s}) = \max_{i=1,2,\dots} R_i W_i(\mathbf{s}), \quad \mathbf{s} \in \mathcal{S} \subset \mathbb{R}^d, \quad (10)$$

where the R_i s are the points of a Poisson process on $(0, \infty)$ with intensity $r^{-2} dr$, and $W_i(\mathbf{s})$ are iid copies of a random process $W(\mathbf{s})$ with $E\{W(\mathbf{s})_+\} = 1$ defined independently of $\{R_i\}$. The functions $X_i(\mathbf{s}) = R_i W_i(\mathbf{s})$ are points of the Poisson process with mean measure Λ defined on an appropriate function space.

3 Modeling

3.1 Construction principles

We broadly distinguish three approaches to building useful max-id models: either by (i) directly specifying the measure Λ in (1) and (3), or (ii) defining the points \mathbf{X}_i constructively in the representation (2), or (iii) exploiting that max-id distributions arise as limits of F_m^m as $m \rightarrow \infty$ where the distributions F_m are not necessarily identical. This last approach was used by Padoan (2013), who obtained a max-id model as the limit of multivariate Gaussian ratios with increasing correlation. We here propose two new general construction principles: in §3.2, we follow (i) by defining a finite measure Λ , while in §3.3, we follow (ii) and define the points \mathbf{X}_i in (2), generalizing the spectral representation of max-stable processes in (10).

A difference between the models defined in §3.2 and §3.3 is that they are based on a finite, respectively infinite, exponent measure Λ . When $\Lambda(E) < \infty$, a finite number N of Poisson points \mathbf{X}_i need to be simulated in the representation (2), and this results in a singularity at the lower endpoint $\boldsymbol{\ell}$ given by $G(\boldsymbol{\ell}) = \exp\{-\Lambda(E)\} > 0$. In practice, this singularity is rather a nuisance than a relevant model feature, and then the measure Λ should be chosen such that the mass $\Lambda(E)$ is large enough to render this singularity negligible. In rare cases, such singularities may occur in data, as for example with long periods (i.e., entire blocks) of dry events with precipitation measurements.

In the following, we focus on developing max-id models able to capture asymptotic independence, a property that max-stable models lack, unless the latter are exactly independent. In §3.3.2, we discuss how to take advantage of a spectral construction generalizing (10) for obtaining max-id models bridging asymptotic dependence and independence.

3.2 Models with finite exponent measure Λ

Using a finite exponent measure $\Lambda = cH$ parametrized by an arbitrary probability distribution H on E and a constant $c > 0$, the max-id vector \mathbf{Z} in (2) has joint distribution $G_{c,H}(\mathbf{z}) = \exp[-c\{1 - H(\mathbf{z})\}]$, $\mathbf{z} \in [\infty, \mathbf{z}]^C$, and margins $G_{c,H,j}(z) = \exp(-c[1 - H_j(z)])$, $z \geq \ell_j$, where H_j denotes the marginal distribution of H with lower endpoint $\ell_j = \sup\{z : H_j(z) = 0\} \in [-\infty, \infty)$, $j = 1, \dots, D$. From the construction (2), \mathbf{Z} can be interpreted as the componentwise maximum over a finite number N of iid events, where N follows the Poisson distribution with mean c . Hence, to simulate the max-id vector \mathbf{Z} , we first sample $N \sim \text{Poisson}(c)$ and then, conditionally on N , we generate $\mathbf{X}_1, \dots, \mathbf{X}_N \stackrel{\text{iid}}{\sim} H$ and set $\mathbf{Z} = \max(\mathbf{X}_1, \dots, \mathbf{X}_N, \boldsymbol{\ell})$. As the event $\{N = 0\}$ has probability $\exp(-c) > 0$, this yields positive mass at the lower boundary $\boldsymbol{\ell}$. In practice, we may restrict c to a range $[c_0, \infty)$ with a relatively large value of $c_0 > 0$, to ensure that $\exp(-c) \approx 0$. Once a parametric model for H has been chosen, the additional parameter c refines the tail behavior of G as compared to H and adds considerable flexibility. Consider the distribution $F = G_{c,H}^{1/m}$ of the original observations, for fixed $m > 0$. Using (5), one obtains

$$1 - F(\mathbf{z}) = 1 - G_{c,H}^{1/m}(\mathbf{z}) = 1 - \exp[-(c/m)\{1 - H(\mathbf{z})\}] \sim (c/m)\{1 - H(\mathbf{z})\}, \quad (11)$$

as $m \rightarrow \infty$ and/or $\min_{j=1, \dots, D} z_j \rightarrow \infty$. For large \mathbf{z} , one has $\{1 - F(\mathbf{z})\}/\{1 - H(\mathbf{z})\} \sim c/m$, and thus the constant c controls the tail weight of F with respect to that of H . Using the approximation (11) in (8) reveals, however, that the asymptotic dependence class of F and

H is the same: the value of χ in (8) is the same for F and H . This property may be useful for modeling, as it gives us a way for constructing new asymptotically (in)dependent max-id models from essentially arbitrary distributions H with the same characteristics.

In the spatial context, the above discussion generalizes to max-id processes constructed as the pointwise maximum $Z(\mathbf{s}) = \max\{X_1(\mathbf{s}), \dots, X_N(\mathbf{s}), \ell(\mathbf{s})\}$, where N is Poisson with mean c , $X_1(\mathbf{s}), \dots, X_N(\mathbf{s}) \stackrel{D}{=} X(\mathbf{s})$ denote iid processes (conditionally on N), and $\ell(\mathbf{s})$ is their lower bound function. Relevant choices for X include Gaussian processes, Student- t processes, or more generally elliptic processes. When X is Gaussian, then Z is asymptotically independent, and when X is Student- t with $\nu > 0$ degrees of freedom, then Z is asymptotically dependent with the max-stable extremal- t limit process (Opitz, 2013).

3.3 Models with infinite exponent measure Λ

3.3.1 Generalized spectral construction

We propose a general approach for constructing max-id vectors with infinite exponent measure by mimicking the spectral representation of max-stable processes in (10), yet with a more flexible definition of the Poisson point process $\{R_i\} > 0$. In §3.3.2, we then advocate a specific parametric model smoothly bridging asymptotic dependence and independence, with a tail structure that resembles the threshold exceedance model of Huser et al. (2017).

To depart from max-stability while staying within the class of max-id processes, we consider the max-stable spectral construction (10) but modify the mean measure κ of the Poisson points $\{R_i\} > 0$. As in (10), let $W_i(\mathbf{s})$ denote iid copies of a random process $W(\mathbf{s})$ with $0 < \mathbb{E}\{W(\mathbf{s})_+\} < \infty$, independent of $\{R_i\}$. Instead of taking $\kappa[r, \infty) = 1/r$, $r > 0$, as in (10), we consider max-id processes constructed as

$$Z(\mathbf{s}) = \max_{i=1,2,\dots} R_i W_i(\mathbf{s}), \quad \mathbf{s} \in \mathcal{S} \subset \mathbb{R}^d, \quad 0 < \{R_i\} \sim \kappa_\gamma, \quad (12)$$

where the measure κ_γ , parametrized by the vector $\gamma \in \Gamma \subset \mathbb{R}^q$, is such that $\kappa_\gamma[0, \infty) = \infty$ but $\kappa_\gamma[r, \infty) < \infty$ for any $r > 0$. We choose κ_γ to contain a specific max-stable model for a parameter subspace. Owing to the infinite number of Poisson points in (12), negative values of $W_i(\mathbf{s})$ do not contribute to the maximum $Z(\mathbf{s})$, and we may replace $W_i(\mathbf{s})$ by its positive part $W_i(\mathbf{s})_+$ and set $\ell = \mathbf{0}$ and $E = [\mathbf{0}, \infty)$. As the exponent measure Λ resulting from (12) must be Radon on $E \setminus \{\ell\}$, we must ensure that

$$\Lambda[\mathbf{0}, \mathbf{z}]^C = \int_0^\infty \{1 - F_{\mathbf{W}}(\mathbf{z}/r)\} \kappa_\gamma(dr) < \infty, \quad \mathbf{z} \in (\mathbf{0}, \infty), \quad (13)$$

where $F_{\mathbf{W}}$ denotes the distribution of the process $W(\mathbf{s})$ observed at any finite collection of $D \geq 1$ sites $\mathbf{s}_1, \dots, \mathbf{s}_D \in \mathcal{S}$. An intuitive interpretation of (12) is to see the max-id process $Z(\mathbf{s})$ as the pointwise maximum of an infinite number of independent ‘‘storms’’ $R_i W_i(\mathbf{s})$ characterized by their amplitude R_i and their spatial extent $W_i(\mathbf{s})$. Apart from the different measure κ_{γ} , a major distinction between the max-stable and max-id constructions in (10) and (12), respectively, is that the assumption of independence between R_i and $W_i(\mathbf{s})$ is essential in (10) while it is not critical in (12). For example, we could choose $W_i(\mathbf{s})$ as a Gaussian process with weakening correlation as the points R_i become larger. We do not pursue this route further in this paper; rather, we focus on choices of κ_{γ} which already lead to a rich class of models.

3.3.2 Sub-asymptotic modeling across dependence classes

The power-law tail in the mean measure κ of the max-stable construction (10) generates asymptotic dependence. To extend this to asymptotic independence, we propose below several lighter-tailed models, with a Pareto tail on the boundary of the parameter space. Similarly to the threshold exceedance models of [Huser et al. \(2017\)](#), our max-id construction shifts focus towards asymptotic independence while comprising the max-stable spectral representation (10) as a special case. We say that a measure κ is Weibull-tailed if

$$\kappa[r, \infty) \sim c r^{\gamma} \exp(-\alpha r^{\beta}), \quad r \rightarrow \infty, \quad (14)$$

for some constants $c > 0$, $\alpha > 0$, $\beta > 0$ and $\gamma \in \mathbb{R}$, where we refer to β as the Weibull coefficient of κ . We propose the following two models for the measure κ_{γ} in (12):

$$\kappa_{\gamma}^{[1]}[r, \infty) = r^{-(1-\alpha)} \exp\{-\alpha(r^{\beta} - 1)/\beta\}, \quad r > 0, \quad \gamma = (\alpha, \beta)^T \in [0, 1) \times [0, \infty), \quad (15)$$

$$\kappa_{\gamma}^{[2]}[r, \infty) = r^{-\beta} \exp\{-\alpha(r^{\beta} - 1)/\beta\}, \quad r > 0, \quad \gamma = (\alpha, \beta)^T \in (0, \infty) \times [0, \infty). \quad (16)$$

For $\beta = 0$, we interpret $\kappa_{\gamma}^{[1]}$ and $\kappa_{\gamma}^{[2]}$ as the continuous limits when $\beta \downarrow 0$, noting that $(r^{\beta} - 1)/\beta \rightarrow \log(r)$ as $\beta \downarrow 0$. We have $\kappa_{\gamma}^{[1]}[r, \infty) = r^{-1}$ and $\kappa_{\gamma}^{[2]}[r, \infty) = r^{-\alpha}$, $r > 0$, as $\beta \downarrow 0$. For each model $k = 1, 2$, $\kappa_{\gamma}^{[k]}$ is a well-defined infinite measure since $\kappa_{\gamma}^{[k]}[r, \infty)$ is the product of two monotonic decreasing functions: an exponential term, which ensures a Weibull tail when $\beta > 0$, and a power law term ensuring $\kappa_{\gamma}^{[k]}[0, \infty) = \infty$, leading to an infinite number of Poisson points. With $\kappa_{\gamma}^{[1]}$, we retrieve the max-stable construction (10) with unit Fréchet margins when $\alpha = 0$ or when $\beta = 0$, provided $E\{W(\mathbf{s})_+\} = 1$. With $\kappa_{\gamma}^{[2]}$, we also get a max-stable model when $\beta = 0$, albeit possessing α -Fréchet marginal distributions.

Specifically, when the process $W(\mathbf{s})$ in (12) is chosen to be a standard Gaussian process, the resulting exponent measures $\Lambda_\gamma^{[k]}$, $k = 1, 2$, satisfy (13) and are Radon measures; see Proposition B.1 in Appendix B. In this case, the max-stable submodel for $\kappa_\gamma^{[1]}$ with $\beta = 0$ or $\alpha = 1$ corresponds to the Schlather process (Schlather, 2002), while we obtain the more flexible extremal- t process with $\alpha > 0$ degrees of freedom with $\kappa_\gamma^{[2]}$ when $\beta = 0$ (Opitz, 2013). Fixing $\alpha = 1$ in $\kappa_\gamma^{[2]}$ yields a more parsimonious one-parameter model, corresponding to the max-stable Schlather process when $\beta = 0$:

$$\kappa_\gamma^{[3]}[r, \infty) = r^{-\beta} \exp \{-(r^\beta - 1)/\beta\}, \quad \gamma = \beta \in [0, \infty). \quad (17)$$

For the max-stable submodels stemming from (15), (16) and (17), we get asymptotic dependence except in the degenerate case of complete independence. In all other non-max-stable cases, the tail decay of $\kappa_\gamma^{[k]}$, $k = 1, 2, 3$, is of Weibull type and yields asymptotic independence with Gaussian $W(s)$; see Proposition B.4 in the Appendix. Under this setting, more information is carried through the so-called coefficient of tail dependence $\eta \in (0, 1]$ (Ledford and Tawn, 1996). By analogy with (8), the latter is defined for a bivariate vector $(Z_1, Z_2)^T$ with unit Fréchet margins through $\chi(z) = \Pr(Z_1 > z \mid Z_2 > z) \sim \mathcal{L}(z)z^{1-1/\eta}$, $z \rightarrow \infty$, where \mathcal{L} denotes a slowly varying function, i.e., $\mathcal{L}(zt)/\mathcal{L}(z) \rightarrow 1$ as $z \rightarrow \infty$, for all fixed $t > 0$. When $\eta = 1$ and $\mathcal{L}(z) \rightarrow \chi > 0$, the vector $(Z_1, Z_2)^T$ is asymptotically dependent; when $\chi(z) \rightarrow 0$, then η captures the rate of decay towards independence. For our proposed models $\kappa_\gamma^{[k]}$, $k = 1, 2, 3$, with parameters leading to asymptotic independence, used in (12) together with a standard Gaussian process $W(\mathbf{s})$ with correlation function $\rho(h)$, the coefficient of tail dependence between two sites $\mathbf{s}_1, \mathbf{s}_2$ at distance $h = \|\mathbf{s}_1 - \mathbf{s}_2\|$ is

$$\eta(h) = [1 + \rho(h)]^{\beta/(\beta+2)}; \quad (18)$$

see Proposition B.4 in Appendix B. The parameter β plays a crucial role for the joint tail decay rate, while the parameter α also impacts the dependence structure of $Z(\mathbf{s})$ for both $\kappa_\gamma^{[1]}$ and $\kappa_\gamma^{[2]}$ but to a milder degree. To illustrate the flexibility of Model (16), Figure 3 displays the bivariate level-dependent extremal coefficient $\theta_2(z) = zV(z, z)$, recall (6), for various parameter values. For $\beta = 0$, the model is max-stable and $\theta_2(z) \equiv \theta_2$ is constant with respect to the level z , whereas for $\beta > 0$, the dependence strength weakens as the level z increases (i.e., $\theta_2(z)$ approaches 2 as $z \rightarrow \infty$). The parameter α modulates the overall dependence strength.

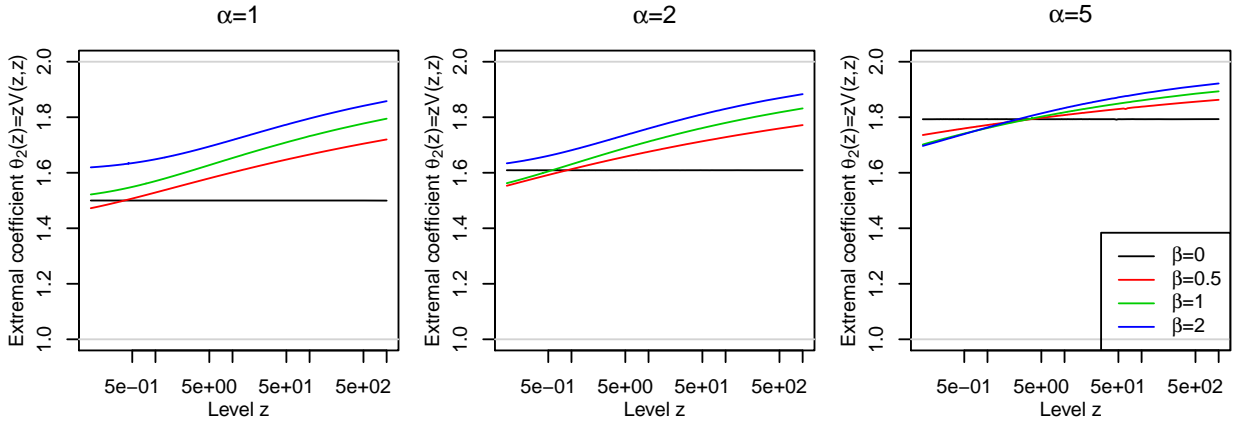


Figure 3: Bivariate level-dependent extremal coefficient $\theta_2(z) = zV(z, z)$, see (6), for Model (16) with $\alpha = 1, 2, 5$ (left to right) and $\beta = 0$ (black), $\beta = 0.5$ (red), $\beta = 1$ (green) and $\beta = 2$ (blue), combined with an underlying standard Gaussian vector $\{W(\mathbf{s}_1), W(\mathbf{s}_2)\}^T$ with correlation $\rho(h) = 0.5$. The level z on the x-axis is on a logarithmic scale.

3.3.3 Simulation of max-id models

When the mean measure of the Poisson point process $\{R_i\}$ in (12) is $\kappa_\gamma[r, \infty) = 1/r$, $r > 0$, yielding a max-stable process with unit Fréchet margins thanks to representation (10), one can simulate the Poisson process $\{R_i\}$ by setting $R_i = 1/U_i$, $i = 1, 2, \dots$, where $\{U_i\}$ denotes the points from a unit rate Poisson process on the positive half-line $(0, \infty)$. A well-known way to generate ordered points $0 < U_1 < U_2 < \dots$ from such a process is to sample a sequence E_1, E_2, \dots of unit exponential random variables and to set $U_i = \sum_{k=1}^i E_k$, $i = 1, 2, \dots$. In this way, the Poisson points R_i are decreasing, which can be exploited in (10) to generate approximate simulations of max-stable processes by truncating the maximum with a predefined accuracy (Schlather, 2002). Furthermore, Schlather (2002) shows that if $W(\mathbf{s}) < C < \infty$ almost surely, then only a finite (but random) number of points R_i needs to be generated for exact simulation of $Z(\mathbf{s})$ in (10). Similarly, to simulate a max-id process defined in (12) with a general mean measure κ_γ , we propose using more general parametric transformations $R_i = T_\gamma(U_i)$ with $T_\gamma : (0, \infty) \rightarrow (0, \infty)$ given as the inverse function of the tail measure $r \mapsto \kappa_\gamma[r, \infty)$ for $r > 0$. When the transformation T_γ is not tractable, approximate simulation of $\{R_i\}$ may be performed in a two-step procedure: first, we generate the number of points N according to a Poisson distribution with mean $\kappa_\gamma[\varepsilon, \infty)$ for small $\varepsilon > 0$. Second, we generate N independent points R_1, \dots, R_N with distribution $F(r) = \kappa_\gamma[\varepsilon, r)/\kappa_\gamma[\varepsilon, \infty)$. We then follow the same algorithm. For the max-id constructions

based on a Gaussian process $W(\mathbf{s})$ in §3.3.2, exact simulation is possible by taking advantage of their elliptical nature; see the details in Proposition B.2 in Appendix B. In the max-stable extremal- t case, such a procedure has been detailed by [Thibaud and Opitz \(2015\)](#).

4 Inference

4.1 Challenges of full likelihood inference

Likelihood inference for max-stable processes is known to be difficult and has been the focus of extensive research during the past decade (see, e.g., [Padoan et al., 2010](#); [Huser and Davison, 2013](#); [Bienvenüe and Robert, 2017](#); [Castruccio et al., 2016](#); [Huser et al., 2016](#); [Dombry et al., 2016](#); [Thibaud et al., 2016](#)). Because max-stable processes and general max-id processes have a similar construction, their joint distributions have essentially the same form, recall (3), and the same challenges arise for max-id processes.

Suppose that n independent replicates of a max-id process $Z(\mathbf{s})$ with unit Fréchet margins, parametrized by a vector $\psi \in \Psi \subset \mathbb{R}^p$, are observed at D sites $\mathbf{s}_1, \dots, \mathbf{s}_D \in \mathcal{S}$, and denote by z_{ij} the i th observation at the j th site, $i = 1, \dots, n$, $j = 1, \dots, D$. Furthermore, suppose that the density of $Z(\mathbf{s})$ with respect to Lebesgue measure on \mathbb{R}^D exists. This holds for the construction (12) (with infinite measure $\kappa_\gamma[0, \infty) = \infty$) when the vector $\mathbf{W} = \{W(\mathbf{s}_1), \dots, W(\mathbf{s}_D)\}^T$ has a density $f_{\mathbf{W}}(\mathbf{w})$ such that the intensity of the Poisson point process $\{R_i \mathbf{W}_i\}$ is obtained as $\lambda(\mathbf{z}) = \int_0^\infty f_{\mathbf{W}}(\mathbf{z}/r) r^{-D} \kappa_\gamma(d\mathbf{r})$. The density of $Z(\mathbf{s})$ never exists for the finite measure model proposed in §3.2 because of the singularity at ℓ , but under appropriate conditions the latter may be neglected and the following discussion still holds for this model when the underlying measure H has a density h ; these issues are further discussed in Appendix A. From (3), the full likelihood function equals

$$L(\psi; \mathbf{z}_1, \dots, \mathbf{z}_n) = \prod_{i=1}^n \left[\exp \{-V(z_{i1}, \dots, z_{iD})\} \sum_{\pi \in \mathcal{P}_D} \prod_{k=1}^K \{-V_{\pi_k}(z_{i1}, \dots, z_{iD})\} \right], \quad (19)$$

where \mathcal{P}_D denotes the collection of all partitions $\pi = \{\pi_1, \dots, \pi_K\}$ of $\mathcal{D} = \{1, \dots, D\}$, and where the exponent function $V(\mathbf{z}) = \Lambda[-\infty, \mathbf{z}]^C$ and its partial derivatives $V_{\pi_k}(\mathbf{z}) = \partial^{|\pi_k|} V(\mathbf{z}) / (\prod_{j \in \pi_k} \partial z_j)$ both depend on the parameter ψ . For large D , the sum in (19) contains too many terms to be computed and the likelihood is intractable ([Castruccio et al., 2016](#)). [Stephenson and Tawn \(2005\)](#) improved the computational and statistical efficiency by conditioning on event times, at the price of introducing bias ([Wadsworth, 2015](#)), and

[Dombry et al. \(2016\)](#) recently showed how to perform likelihood inference for max-stable processes in larger dimensions based on a stochastic Expectation-Maximization algorithm, but their approach remains fairly demanding in moderately high dimensions.

Another challenge for certain models is linked to the computation of $V(\mathbf{z})$ and $V_{\pi_k}(\mathbf{z})$. Appendix A gives general expressions of these functions for the finite and infinite measure models introduced in §3.2 and §3.3, respectively, and discusses related difficulties. In the next section, we describe pairwise likelihood inference, which allows us to significantly reduce the computational burden while maintaining satisfactory statistical efficiency.

4.2 Pairwise likelihood approach

Pairwise likelihood inference for max-stable processes has been popularized by [Padoan et al. \(2010\)](#). This approach naturally extends to max-id processes. Instead of maximizing (19), pairwise likelihood inference relies on

$$PL(\boldsymbol{\psi}; \mathbf{z}_1, \dots, \mathbf{z}_n) = \prod_{1 \leq j_1 < j_2 \leq D} [L\{\boldsymbol{\psi}; (z_{1j_1}, z_{1j_2})^T, \dots, (z_{nj_1}, z_{nj_2})^T\}]^{\omega_{j_1;j_2}}, \quad (20)$$

where the innermost term is the bivariate likelihood computed from (19), with each independent contribution given by $L(\boldsymbol{\psi}; (z_{ij_1}, z_{ij_2})^T) = \exp\{-V(z_{ij_1}, z_{ij_2})\}\{V_1(z_{ij_1}, z_{ij_2})V_2(z_{ij_1}, z_{ij_2}) - V_{12}(z_{ij_1}, z_{ij_2})\}$, and where $\omega_{j_1;j_2} \geq 0$ denotes a nonnegative weight attributed to this contribution. By carefully choosing binary weights, i.e., $\omega_{j_1;j_2} \in \{0, 1\}$, one can reduce the number of pairs involved in (20) to improve computations and efficiency. Usually, weights are fixed according to distance: $\omega_{j_1;j_2} = 1$ if $\|\mathbf{s}_1 - \mathbf{s}_2\| < \delta$, where $\delta > 0$ is a suitable cut-off distance and $\omega_{j_1;j_2} = 0$ otherwise ([Padoan et al., 2010](#); [Bevilacqua et al., 2012](#)).

As the dependence between pairs is neglected in (20), classical likelihood theory does not apply. However, because pairwise likelihoods are constructed from valid likelihood terms, they retain appealing properties under mild conditions, including consistency and asymptotic normality ([Varin et al., 2011](#)). Denote by $\hat{\boldsymbol{\psi}}$ the maximum pairwise likelihood estimator and by $\boldsymbol{\psi}_0 \in \Psi \subset \mathbb{R}^p$ the true parameter value. Under regularity conditions ([Padoan et al., 2010](#)), and provided that $\boldsymbol{\psi}$ is identifiable from the bivariate densities, one has the following large sample behavior:

$$n^{1/2}(\hat{\boldsymbol{\psi}} - \boldsymbol{\psi}_0) \xrightarrow{D} \mathcal{N}_p(\mathbf{0}, \mathbf{J}^{-1} \mathbf{K} \mathbf{J}^{-1}), \quad (21)$$

where $n^{-1} \mathbf{J}^{-1} \mathbf{K} \mathbf{J}^{-1}$ is known as the sandwich matrix with $\mathbf{J} = \mathbb{E} \left\{ -\frac{\partial^2}{\partial \boldsymbol{\psi} \partial \boldsymbol{\psi}^T} \log PL(\boldsymbol{\psi}_0; \mathbf{Z}) \right\}$ and $\mathbf{K} = \text{var} \left\{ \frac{\partial}{\partial \boldsymbol{\psi}} \log PL(\boldsymbol{\psi}_0; \mathbf{Z}) \right\}$. Model comparison may be performed using the com-

posite likelihood information criterion (CLIC) defined as $\text{CLIC} = -2 PL(\hat{\psi}; \mathbf{z}_1, \dots, \mathbf{z}_n) + 2 \text{trace}(\hat{\mathbf{J}}^{-1} \hat{\mathbf{K}})$, where $\hat{\mathbf{J}}$ and $\hat{\mathbf{K}}$ are estimators of \mathbf{J} and \mathbf{K} , respectively. The rescaled version CLIC^* (Davison and Gholamrezaee, 2012), based on $C^{-1} PL(\hat{\psi}; \mathbf{z}_1, \dots, \mathbf{z}_n)$ with $Q = 2D^{-1} \sum_{1 \leq j_1 < j_2 \leq D} \omega_{j_1, j_2}$, is easier to interpret since it recognizes that all variables in (20) appear on average Q times more often than they should in case of independence. When $\omega_{j_1, j_2} = 1$ for all $1 \leq j_1 < j_2 \leq D$, then $Q = D - 1$.

4.3 Simulation study

To validate our pairwise likelihood inference approach detailed in §4.2, we first consider the parsimonious model (17) combined with a standard Gaussian process $W(\mathbf{s})$ in (12). We simulate $n = 50$ independent replicates of the max-id model at $D = 10, 15, 20, 30$ sites uniformly generated in $\mathcal{S} = [0, 1]^2$, considering $\beta = 0$ (Schlather max-stable model) and $\beta = 0.5, 1, 2$ (asymptotically independent max-id models), and taking an isotropic exponential correlation function $\rho(h) = \exp(-h/\lambda)$ with range parameter $\lambda = 0.5$ for the process $W(\mathbf{s})$. We then estimate $\psi = (\beta, \lambda)^T \in \Psi = [0, \infty) \times (0, \infty)$ using the pairwise likelihood estimator based on (20) with binary weights and cut-off distance $\delta = 0.5$. More precisely, we perform two separate iterative maximizations of (20), one with $\beta = 0$ fixed and one with $\beta \geq 0$ free, and then compare the maximized pairwise likelihoods to determine the optimal value of β . Boxplots of estimated parameters, based on $R = 1000$ Monte Carlo simulations, are displayed in Figure 4. They suggest that the pairwise likelihood estimator performs quite well overall and it improves slightly as the number of sites D increases. However, the computational cost increases quadratically with D as the cut-off distance δ is kept fixed.

Further simulation results based on the more flexible model (16), where α , β and λ are jointly estimated, are reported in the Supplementary Material. Results show that the pairwise likelihood estimator performs quite well overall, although the difficulty in identifying α and β leads to relatively high estimation variability when α or β are large.

To assess the impact of wrongfully assuming max-stability when the data are max-id but asymptotically independent, we consider the same setting as above with $\alpha = 1$ fixed, $\beta = 0, 0.5, 1, 2$, exponential correlation function with range $\lambda = 0.5$, $D = 30$ sites in $[0, 1]^2$ and $n = 50$ replicates. Table 1 reports the mean difference between the maximized pairwise log-likelihoods obtained with $\beta \geq 0$ estimated from the data and with $\beta = 0$ held fixed (i.e., the model is assumed to be max-stable). We also report (i) the true tail probability

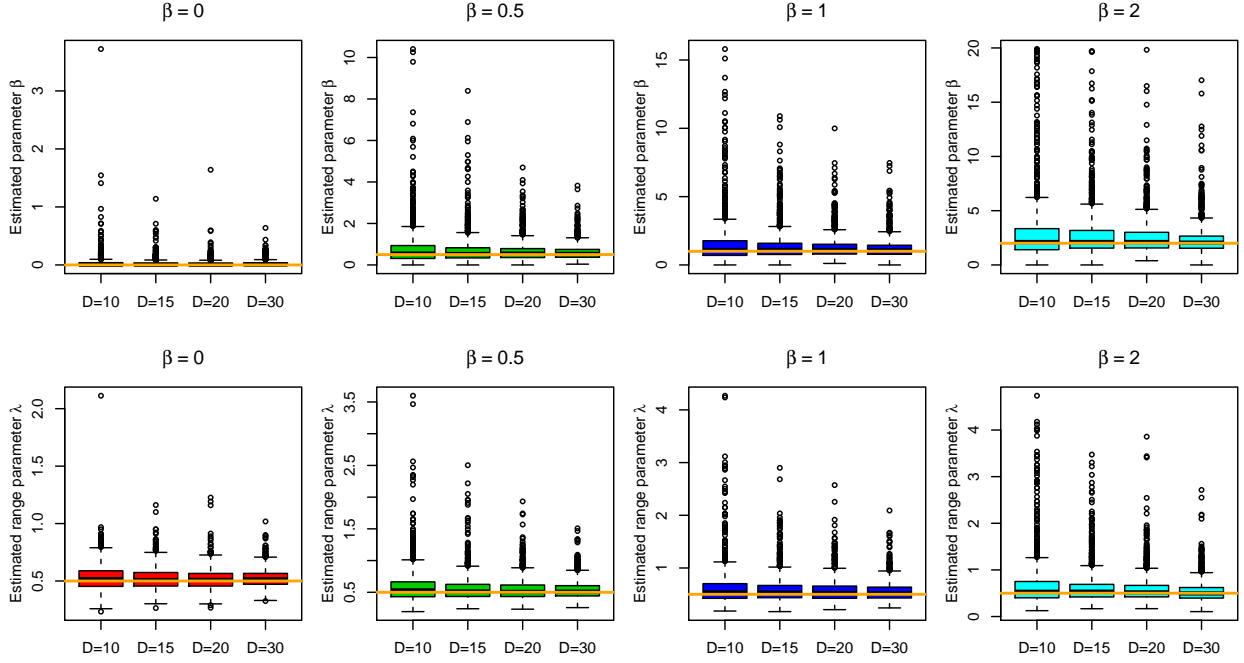


Figure 4: Boxplots of estimated parameters $\hat{\beta}$ (top) and $\hat{\lambda}$ (bottom) for max-id data simulated according to model (17) with $\beta = 0, 0.5, 1, 2$ (left to right) at $D = 10, 15, 20, 30$ sites randomly generated in $[0, 1]^2$, with $n = 50$ independent replicates. The pairwise likelihood estimator maximizing (20) with binary weights and cut-off distance $\delta = 0.5$ was used. True values are indicated by orange horizontal lines. 1000 Monte Carlo simulations were performed.

$p(z) = 1 - \Pr\{Z(\mathbf{s}_1) \leq z, \dots, Z(\mathbf{s}_{36}) \leq z\}$ that at least one of 36 grid points $\mathbf{s}_1, \dots, \mathbf{s}_{36} \in \{0, 0.2, \dots, 1\}^2$ experiences an exceedance of the level z fixed to the 99%-quantile, (ii) its mean estimate $\hat{p}_i(z) = R^{-1} \sum_{r=1}^R \hat{p}_{i;r}(z)$ (where $\hat{p}_{i;r}(z)$ is the estimate for the r th simulation), $i = 1, 2$, based on the model with $\beta = 0$ fixed and $\beta \geq 0$ estimated, respectively, and (iii) the mean relative errors $E_i = R^{-1} \sum_{r=1}^R |\hat{p}_{i;r}(z) - p(z)|/p(z)$, $i = 1, 2$. Notice that $p(z)$ denotes the probability that the marginal 100-year return level is exceeded at at least one of the 36 selected locations, and that $1/p(z)$ is the return period of the corresponding spatial extreme event. Thus, one must have $0.01 \leq p(z) \leq 1 - 0.99^{36} \approx 0.30$, with the lower and upper bounds corresponding to perfect dependence and independence, respectively. The results reported in Table 1 strongly suggest that incorrectly specifying the dependence structure to be max-stable might have dramatic implications in terms of joint tail estimation under asymptotic independence, while our proposed max-id models are flexible enough to give reliable results even in the boundary max-stable case.

Table 1: Performance of max-stable and non-max-stable models constructed from (12), with a standard Gaussian process $W(\mathbf{s})$ with correlation $\rho(h) = \exp(-h/\lambda)$ and a Poisson point process $\{R_i\}$ with measure (17) with $\beta = 0, 0.5, 1, 2$. Data were simulated at $D = 30$ sites randomly generated in $[0, 1]^2$ with $n = 50$ replicates, and parameters were estimated using the pairwise likelihood estimator (20) taking pairs at maximum distance $\delta = 0.5$. We report (1st row) the difference $\widehat{p\ell}_2 - \widehat{p\ell}_1$ in maximized log-pairwise likelihood under the model with $\beta \geq 0$ estimated and with $\beta = 0$ fixed, averaged over $R = 1000$ simulations, (2nd row) the true tail probability $p(z) = 1 - \Pr\{Z(\mathbf{s}_1) \leq z, \dots, Z(\mathbf{s}_{36}) \leq z\}$ with $\mathbf{s}_1, \dots, \mathbf{s}_{36} \in \{0, 0.2, \dots, 1\}^2$ and z as the 99%-quantile, and (3rd–4th rows) the mean estimate $\widehat{p}_i(z) = R^{-1} \sum_{r=1}^R \widehat{p}_{i;r}(z)$, $i = 1, 2$, of $p(z)$ based on the model with $\beta = 0$ fixed and $\beta \geq 0$ estimated, respectively. Values in parentheses are mean relative errors $E_i = R^{-1} \sum_{r=1}^R |\widehat{p}_{i;r}(z) - p(z)|/p(z)$, $i = 1, 2$.

	$\beta = 0$	$\beta = 0.5$	$\beta = 1$	$\beta = 2$
$\widehat{p\ell}_2 - \widehat{p\ell}_1$	7.3	113.0	157.7	178.5
True tail probability $p(z)$	0.041	0.076	0.097	0.122
$\widehat{p}_1(z)$ with $\beta = 0$ fixed	0.041 (3.0%)	0.045 (40.8%)	0.047 (51.0%)	0.050 (59.2%)
$\widehat{p}_2(z)$ with $\beta \geq 0$ estimated	0.044 (7.4%)	0.076 (8.6%)	0.095 (6.3%)	0.120 (5.5%)

5 Analysis of Dutch wind gusts

Daily weed gust extremes from the Netherlands were analyzed by [Opitz \(2016\)](#) using an asymptotically independent Laplace random field model for high threshold exceedances. We here reanalyze these data by adopting a block maximum approach and fitting our proposed max-id model (16) and its max-stable counterpart. The original dataset contains 3241 daily maxima collected at 30 monitoring stations across the Netherlands from November 11, 1999, to November 13, 2008. Unlike [Opitz \(2016\)](#), we remove non-stationary seasonal effects by focusing on data from the months October–March, which experience the strongest wind gusts. More details on the original data and the location of monitoring stations may be found in [Opitz \(2016\)](#) and the references therein. To study wind gust extremes on various time scales, we then compute weekly, monthly and yearly block maxima, making sure that observations within these blocks are consecutive in time. This yields 1594, 220, 52 and 8 maxima per site for the daily, weekly, monthly and yearly time scales, respectively.

We model marginal distributions separately at each location, but jointly across time scales to borrow strength across time series when few observations are available. Specifically, let $z_{ij;k}$ denote the i th observation at the j th monitoring station for the k th time scale. We assume that the daily maxima, $z_{ij;1}$, follow a generalized extreme-value (GEV) distribution $G_{j;1}(z)$ with location, scale and shape parameters $\mu_j \in \mathbb{R}$, $\sigma_j > 0$ and $\xi_j \in \mathbb{R}$, respectively,

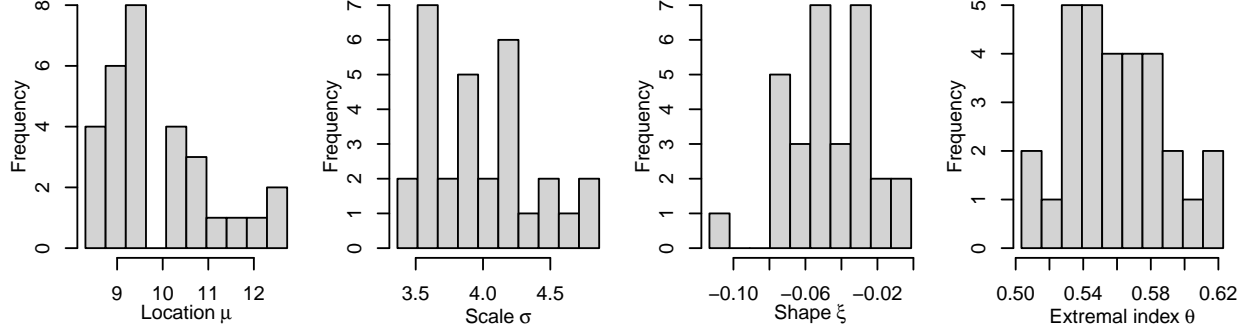


Figure 5: Histograms of estimated marginal GEV parameters for all monitoring stations.

and that maxima for larger time scales, $z_{ij;k}$, are also GEV-distributed according to

$$G_{j;k}(z) = G_{j;1}(z)^{b_k \theta_j} = \exp \left\{ - \left(1 + \xi_j \frac{z - [\mu_j - \sigma_j \{1 - (b_k \theta_j)^{\xi_j}\} / \xi_j]}{\sigma_j (b_k \theta_j)^{\xi_j}} \right)_+^{-1/\xi_j} \right\}, \quad k = 2, 3, 4,$$

where $a_+ = \max(0, a)$, b_k , $k = 2, 3, 4$, refers to the (approximate) block size for weekly, monthly and yearly data, respectively, and $\theta_j \in (0, 1]$ is the extremal index specific to each station, representing the proportion of independent extremes within each block. Here, we set $b_2 = 7$, $b_3 = 30$ and $b_4 = 182$. Figure 5 displays histograms of the four estimated parameters $(\hat{\mu}_j, \hat{\sigma}_j, \hat{\xi}_j, \hat{\theta}_j)^T$ for all sites. In particular, the estimated shape parameters are all negative, suggesting short bounded tails, and the extremal index roughly lies in the interval $[0.5, 0.6]$, revealing some mild extremal dependence in the daily time series. Quantile-quantile plots (not shown) suggest that the fits are good overall at all sites and time scales.

The special dependence structure of componentwise maxima suggests that these data might be well described over space by a max-id process. Although we expect the max-stability property to be reasonable for large block sizes such as for yearly maxima, it might be dubious for small block sizes such as for daily maxima. Figure 1 illustrates this by showing the empirical level-dependent extremal coefficient $\theta_D(z)$, recall (6), for the daily, weekly and monthly wind gust maxima computed over the $D = 30$ stations; as $\theta_D(z)$ appears to be increasing rather than constant with z , this casts some doubt on the validity of the max-stable assumption. Treating the estimated margins as exact, we then fit several max-id models constructed from (12) using an isotropic Gaussian process $W(\mathbf{s})$ with powered exponential correlation function $\rho(h) = \exp\{-(h/\lambda)^\nu\}$, $h \geq 0$, with range $\lambda > 0$ and smoothness $\nu \in (0, 2]$, and using the Poisson point process mean measure proposed in (16), which depends on the parameters $\alpha > 0$ and $\beta \geq 0$. We consider four max-id models, fitted separately for

Table 2: Fitting of the max-id model constructed from (12) and (16) to the Dutch wind gust maxima. Parameters α , β , $\log(\lambda)$ and ν were estimated for the (top left) Schlather max-stable model ($\alpha = 1$, $\beta = 0$), (top right) extremal- t max-stable model ($\beta = 0$), (bottom left) max-id model (17) ($\alpha = 1$), and (bottom right) unconstrained max-id model (16). Different rows correspond to different time scales. Model estimation was performed by maximum pairwise likelihood, with binary weights and maximum distance 100km between selected pairs. The CLIC*, recall Section 4.2, is reported in the right-most column of each sub-table. For a fixed dataset, a lower CLIC* indicates a better model.

Time scale	Schlather max-stable model				Extremal- t max-stable model				CLIC*	
	α	β	$\log(\hat{\lambda})$	$\hat{\nu}$	$\hat{\alpha}$	β	$\log(\hat{\lambda})$	$\hat{\nu}$		
Daily	1	0	8.93	0.46	-42419.9	4.70	0	12.07	0.46	-44341.5
Weekly	1	0	8.63	0.40	-5093.8	4.57	0	12.16	0.40	-5371.3
Monthly	1	0	7.02	0.42	-791.0	3.29	0	9.69	0.43	-831.5
Yearly	1	0	6.11	0.33	-73.4	1.22	0	6.76	0.32	-73.4

Time scale	Parsimonious max-id model (17)				General max-id model (16)				CLIC*	
	α	$\hat{\beta}$	$\log(\hat{\lambda})$	$\hat{\nu}$	$\hat{\alpha}$	$\hat{\beta}$	$\log(\hat{\lambda})$	$\hat{\nu}$		
Daily	1	1.79	10.86	0.46	-44909.8	2.69	1.40	11.12	0.48	-45086.1
Weekly	1	1.68	9.49	0.49	-5438.8	2.57	1.29	11.33	0.40	-5466.4
Monthly	1	1.37	8.80	0.43	-833.6	2.28	0.58	8.54	0.48	-836.4
Yearly	1	0.17	7.15	0.27	-73.5	1.13	0.02	6.39	0.35	-73.8

each time scale: $\alpha = 1$ fixed and $\beta = 0$ fixed (Schlather max-stable model); $\alpha > 0$ and $\beta = 0$ fixed (extremal- t max-stable model with α degrees of freedom); $\alpha = 1$ fixed and $\beta \geq 0$ (our proposed parsimonious model (17)); $\alpha > 0$ and $\beta \geq 0$ (our most general max-id model (16)).

All models were estimated by maximizing the pairwise likelihood (20), considering all pairs of locations less than $\delta = 100$ km apart (i.e., keeping roughly 40% of possible pairs). For the most complex max-id model, a single fit took about 30min, 3.5h, 15h, and 4 days for yearly, monthly, weekly and daily maxima, respectively, on a workstation with 20 cores exploited for computing the pairwise likelihood in parallel. Table 2 reports the results. Overall, the large estimated range parameter $\hat{\lambda}$ suggests that spatial dependence is quite strong, while the estimated smoothness parameter $\hat{\nu} < 0.5$ shows that there is small-scale variability, as might be expected with wind gusts. A quick inspection of the estimated parameters for the Schlather model suggests that the max-stability assumption might be dubious for these data: the range λ and the smoothness ν are both decreasing with larger time scales, suggesting a weakening of spatial dependence as wind gusts become more extreme. The results for the extremal- t model seem to confirm this, although the parameter α has the

opposite effect. More affirmative conclusions can be drawn by comparing the fits of the max-id models (16) and (17) with their max-stable counterparts, the latter obtained by fixing $\beta = 0$. For yearly maxima, the estimated β parameter is fairly close to zero in both non-max-stable models; unreported results for model (16) confirm that an asymptotic 95% confidence interval for β includes 0, suggesting that the max-stable assumption is reasonable in this case. Furthermore, the CLIC* values are all very similar for yearly maxima, suggesting that the simplest Schlather max-stable model might be appropriate here. By contrast, for daily, weekly and monthly maxima, the estimated β parameter in non-max-stable models is always quite far from zero; unreported results show that β is indeed always significantly different from zero at the 95% confidence level. Moreover, the CLIC* values are strongly supporting the more flexible non-max-stable models, especially for daily maxima. Overall, according to the CLIC*, non-max-stable models outperform their max-stable counterparts, and the most complex max-id model (16) performs better than the parsimonious model (17). Interestingly, in both max-id models (16) and (17), the estimated β parameter decreases monotonically to zero as the block size becomes larger, which implies that these block maxima tend to behave more and more like a max-stable process as the block size increases; this is expected from classical asymptotic results of Extreme-Value Theory, while the additional β parameter provides extra flexibility at sub-asymptotic regimes characterized by small block sizes.

To assess the goodness-of-fit, Figure 6 displays empirical and fitted extremal coefficients $\theta_D(z)$ for monthly and weekly maxima, for three subsets of sites of dimension $D = 5$ at various distances. We compare the fits of the max-stable extremal- t model with our proposed max-id model (16). Unlike the quite rigid extremal- t model, our asymptotically independent max-id model can capture weakening of dependence, although there still is room for improvement on a weekly time scale. More flexible max-id models could be designed for example by allowing for spatial anisotropy or by choosing processes $W_i(\mathbf{s})$ in the spectral construction (12) that depend on the Poisson points R_i , which might further improve results. Overall, the CLIC* values, the estimated parameters (Table 2) and the model diagnostics suggest that our max-id model outperforms the max-stable extremal- t counterpart.

6 Discussion

We have proposed a new family of sub-asymptotic spatial models for block maxima, that are more flexible than max-stable processes while remaining max-infinitely divisible. In

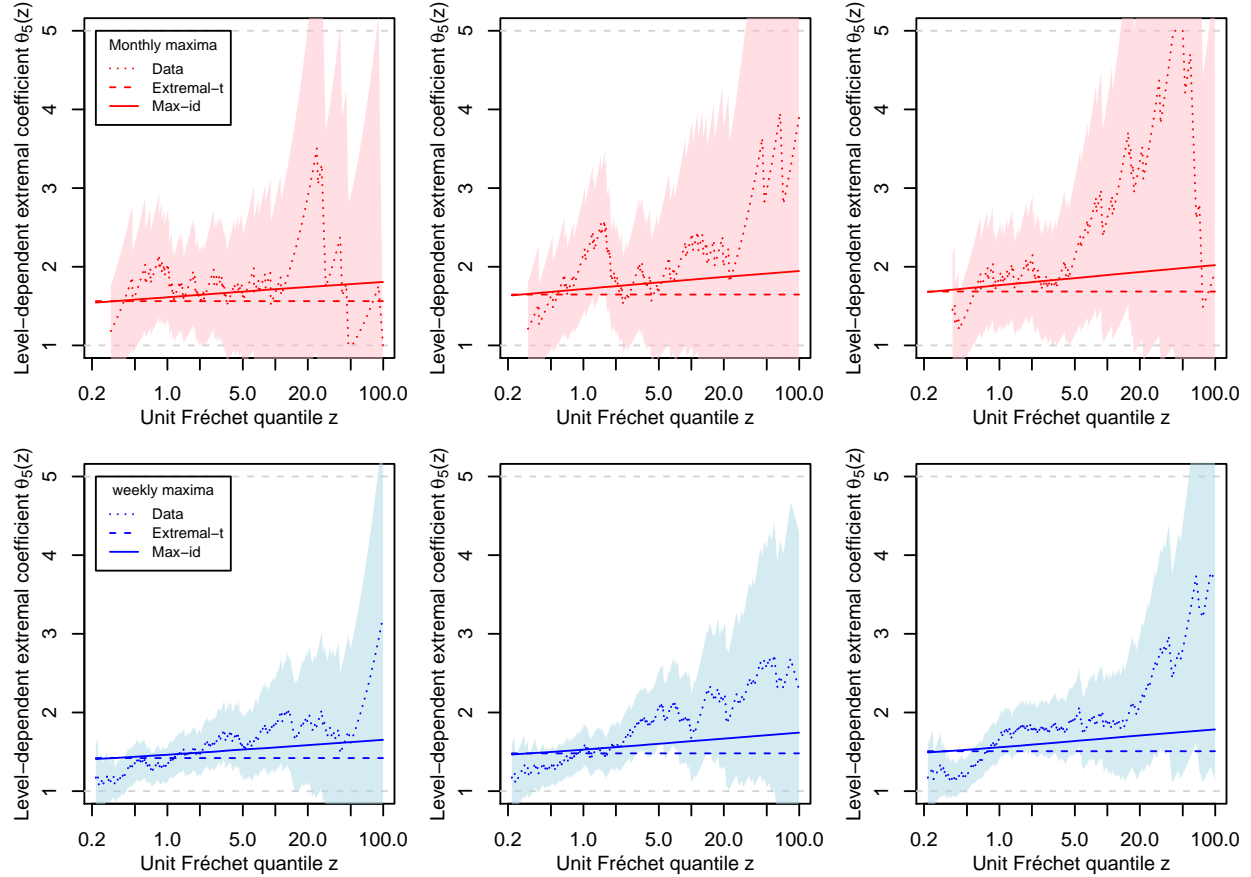


Figure 6: Level-dependent extremal coefficients $\theta_D(z)$, plotted with respect to unit Fréchet quantile z (on a log scale), for monthly maxima (top) and weekly maxima (bottom) for three subsets of sites of dimension $D = 5$ at average distance 33km (left), 57km (middle) and 74km (right). Dotted lines are empirical estimates with 95% pointwise confidence bands (shaded areas), while solid and dashed lines are the fitted coefficients based on the max-id model (16) and the extremal- t max-stable model, respectively.

particular, we have developed a general constructive approach that extends the spectral characterization of max-stable processes, using an infinite number of independent replicates of a random process of the form $RW(\mathbf{s})$ to build asymptotically independent max-id structures. In our examples, we took the process $W(\mathbf{s})$ to be Gaussian and independent of the random scale R for simplicity. Preliminary experiments suggest that flexible dependence structures may also be obtained by letting $W(\mathbf{s})$ depend on R in such a way that the correlation strength of the W process decreases as R increases. We plan to investigate such max-id models in future research.

Another interesting research direction would be to formulate a Bayesian max-id model based on (16), in which a prior distribution for the parameter $\beta \geq 0$ would be chosen to

shrink max-id models towards their “simpler” max-stable counterparts arising for $\beta = 0$. One could take advantage of the concept of penalized-complexity priors (Simpson *et al.*, 2017), or alternatively assume that the prior for β is a mixture between a continuous distribution on $(0, \infty)$ and a point mass at zero. Implementation of the Bayesian fitting procedure for max-id processes could mimic the approach of Thibaud *et al.* (2016) for max-stable processes.

The max-id framework may be used to provide natural models for maxima of discrete data, such as binary observations or counts. Many of the standard distributions (Poisson, etc.) do not lead to valid univariate max-stable limits. Moreover, pretransformation of margins and max-stable dependence modeling may be awkward by disregarding the discrete support of data. We plan to explore this further in future research.

A Likelihood formulae

A.1 Likelihood for finite measure max-id model

The construction of §3.2, has finite exponent measure $\Lambda = cH$, and we obtain $V(\mathbf{z}) = c\{1 - H(\mathbf{z})\}$. If the distribution H has a density h , one has $V_{\pi_k}(\mathbf{z}) = -cH_{\pi_k}(\mathbf{z})$, $|\pi_k| \geq 1$, where subscripts denote partial differentiation. In particular, $V_{\mathcal{D}}(\mathbf{z}) = -ch(\mathbf{z})$. In the case where H is the multivariate standard Gaussian distribution $\Phi_D(\cdot; \Sigma)$ with correlation matrix Σ and density $\phi_D(\cdot; \Sigma)$, these expressions become

$$V(\mathbf{z}) = c\{1 - \Phi_D(\mathbf{z}; \Sigma)\}; \quad (22)$$

$$V_{\pi_k}(\mathbf{z}) = -c\Phi_{D-|\pi_k|}(\mathbf{z}; \Sigma_{\pi_k^C; \pi_k^C} - \Sigma_{\pi_k^C; \pi_k} \Sigma_{\pi_k; \pi_k}^{-1} \Sigma_{\pi_k; \pi_k^C}) \phi_{|\pi_k|}(\mathbf{z}; \Sigma_{\pi_k; \pi_k}), \quad 1 \leq |\pi_k| < D; \quad (23)$$

$$V_{\mathcal{D}}(\mathbf{z}) = -c\phi_D(\mathbf{z}; \Sigma), \quad (24)$$

where $\Sigma_{A; B}$ denotes the matrix Σ restricted to the rows in the set A and columns in B , and $\pi_k^C = \mathcal{D} \setminus \pi_k$. Expressions (22) and (23) involve the multivariate Gaussian distribution in dimension D and $D - |\pi_k|$, respectively, which may be approximated using quasi Monte Carlo methods. It remains expensive to compute when D is moderately large, which is a common issue with most popular spatial extreme-value models. The finiteness of Λ entails a point mass at the lower boundary $\boldsymbol{\ell}$, and therefore the likelihood (19) needs to be modified accordingly as $L_{H,c}(\boldsymbol{\psi}; \mathbf{z}_1, \dots, \mathbf{z}_n) = \exp(-cm) \times L(\boldsymbol{\psi}; \mathbf{z}_i, i \in \mathcal{I})$, where $\mathcal{I} = \{i \in \{1, \dots, n\} : \mathbf{z}_i > \boldsymbol{\ell}\}$ and $m = n - |\mathcal{I}|$ is the number of vectors \mathbf{z}_i equal to the lower boundary $\boldsymbol{\ell}$. In practice, events are typically not observed at the lower boundary, which induces bias since

the likelihood wrongfully reduces to (19) when $m = 0$. To limit this nuisance, one can assume that $c > c_0 > 0$, with c_0 large, or adopt a censored likelihood approach with a low threshold.

A.2 Likelihood for infinite measure max-id model

For the generalized spectral construction proposed in §3.3, we adopt a bottom-up approach to derive the expression for $V(\mathbf{z})$ and $V_{\pi_k}(\mathbf{z})$. Using the independence of $\{R_i\}$ and $\{\mathbf{W}_i\}$, we can deduce that the intensity of the Poisson point process $\{\mathbf{X}_i\} = \{R_i \mathbf{W}_i\}$, stemming from (12) when the process is observed at D sites, is

$$\lambda(\mathbf{z}) = \int_0^\infty f_W(\mathbf{z}/r) r^{-D} f(r) dr, \quad \mathbf{z} \in \mathbb{R}^D, \quad (25)$$

where f_W denotes the density of \mathbf{W}_i and $f(r) = -d\kappa_\gamma[r, \infty)/dr$ is the intensity of the Poisson point process $\{R_i\}$, provided the latter exist. For the models $\kappa_\gamma^{[1]}$, $\kappa_\gamma^{[2]}$ and $\kappa_\gamma^{[3]}$ defined in (15), (16) and (17), respectively, the intensity $f(r)$ may be expressed as

$$f^{[1]}(r) = \{(1 - \alpha)r^{\alpha-2} + \alpha r^{\alpha+\beta-2}\} \exp\{-\alpha(r^\beta - 1)/\beta\}, \quad r > 0; \quad (26)$$

$$f^{[2]}(r) = (\beta r^{-\beta-1} + \alpha r^{-1}) \exp\{-\alpha(r^\beta - 1)/\beta\}, \quad r > 0; \quad (27)$$

$$f^{[3]}(r) = (\beta r^{-\beta-1} + r^{-1}) \exp\{-(r^\beta - 1)/\beta\} \quad r > 0. \quad (28)$$

Using $V(\mathbf{z}) = \Lambda[-\infty, \mathbf{z}]^C = \int_{[-\infty, \mathbf{z}]^C} \lambda(\mathbf{x}) d\mathbf{x}$, one has the following relationships:

$$V(\mathbf{z}) = \int_0^\infty \{1 - F_W(\mathbf{z}/r)\} f(r) dr; \quad (29)$$

$$V_{\pi_k}(\mathbf{z}) = - \int_0^\infty F_{W; \pi_k}(\mathbf{z}/r) r^{-|\pi_k|} f(r) dr; \quad (30)$$

$$V_D(\mathbf{z}) = - \int_0^\infty f_W(\mathbf{z}/r) r^{-D} f(r) dr, \quad (31)$$

where F_W is the distribution of \mathbf{W}_i and $F_{W; \pi_k}(\mathbf{w}) = \partial^{|\pi_k|} F_W(\mathbf{w}) / (\prod_{j \in \pi_k} \partial w_j)$ are its partial derivatives. If \mathbf{W}_i is multivariate standard Gaussian with correlation matrix Σ , then $F_W(\mathbf{w}) = \Phi_D(\mathbf{w}; \Sigma)$, $f_W(\mathbf{w}) = \phi_D(\mathbf{w}; \Sigma)$ and $F_{W; \pi_k}(\mathbf{w}) = \Phi_{D-|\pi_k|}(\mathbf{w}; \Sigma_{\pi_k^C; \pi_k^C} - \Sigma_{\pi_k^C; \pi_k} \Sigma_{\pi_k; \pi_k}^{-1} \Sigma_{\pi_k; \pi_k^C} \phi_{|\pi_k|}(\mathbf{w}; \Sigma_{\pi_k; \pi_k}))$. As in (22) and (23), the expressions (29) and (30) rely on the computation of the multivariate Gaussian distribution in dimension D and $D - |\pi_k|$, respectively, which can be quite demanding for large D . The unidimensional integrals in (29), (30) and (31) are not always available in closed form, e.g., when considering our proposed models $f^{[1]}(r)$, $f^{[2]}(r)$ and $f^{[3]}(r)$ in (26), (27) and (28), respectively. Standard numerical methods can be used to approximate them accurately, at the price of an increased computational burden, similarly to [Huser et al. \(2017\)](#).

B Results for the Gaussian-based constructions

Proposition B.1 (Well-definedness).

The construction $Z(\mathbf{s}) = \max_{i=1,2,\dots} R_i W_i(\mathbf{s})$ with $\{R_i\}$ the points of a Poisson process distributed according to one of the intensity measures $\kappa_{\gamma}^{[k]}$, given for $k = 1, 2, 3$ in (15), (16) and (17) respectively, and with $W_i(\mathbf{s})$ iid copies of a standard Gaussian process independent of $\{R_i\}$, yields a well-defined max-id process.

Proof. Observe that $\kappa_{\gamma}^{[k]}$ are infinite measures on the positive half-line and $\Pr\{W_i(\mathbf{s}) > 0\} > 0$, such that $\Pr\{Z(\mathbf{s}) > 0\} = 1$, and we can focus on positive values of $Z(\mathbf{s})$. The construction of $Z(\mathbf{s})$ as the pointwise maximum over a Poisson process yields a valid max-id process, provided that all values of the multivariate exponent function, formally defined as

$$V(\mathbf{z}) = \Lambda_{\gamma}^{[k]}[-\infty, \mathbf{z}]^C = \int_0^{\infty} (1 - F_{\mathbf{W}}(\mathbf{z}/r)) \kappa_{\gamma}^{[k]}(dr), \quad \mathbf{z} > \mathbf{0}, \quad k = 1, 2, 3, \quad (32)$$

are finite for any standard D -dimensional Gaussian vector \mathbf{W} .

Using Mill's ratio for the univariate standard Gaussian distribution with density ϕ , the multivariate standard Gaussian tail probability $1 - F_{\mathbf{W}}(\mathbf{x})$ can be bounded above by $(1 + \varepsilon_W)D\phi(\min_{j=1,\dots,D} x_j) \min_{j=1,\dots,D} x_j$ as $\min x_j \rightarrow \infty$ with suitably fixed $\varepsilon_W > 0$. Therefore, we can fix a constant $c_W > 0$ such that $1 - F_{\mathbf{W}}(\mathbf{x}) < c_W \phi(\min_{j=1,\dots,D} x_j) \min_{j=1,\dots,D} x_j$ for all $\mathbf{x} > \mathbf{0}$. In the decomposition

$$V(\mathbf{z}) = \int_0^1 (1 - F_{\mathbf{W}}(\mathbf{z}/r)) \kappa_{\gamma}^{[k]}(dr) + \int_1^{\infty} (1 - F_{\mathbf{W}}(\mathbf{z}/r)) \kappa_{\gamma}^{[k]}(dr),$$

the second term on the right hand side is finite, and it remains to prove finiteness of the first term. By using the upper bound on the multivariate Gaussian tail probability, collecting all constant terms in a constant C and writing $z = \min_{j=1,\dots,D} z_j$, we get

$$\begin{aligned} \int_0^1 (1 - F_{\mathbf{W}}(\mathbf{z}/r)) \kappa_{\gamma}^{[k]}(dr) &\leq Cz \int_0^1 \exp\{-z^2/(2r^2)\} r^{-1} f^{[k]}(r) dr \\ &\stackrel{r \rightarrow 1/r}{=} Cz \int_1^{\infty} \exp(-z^2 r^2/2) r^{-1} f^{[k]}(1/r) dr. \end{aligned}$$

The term $\exp(-z^2 r^2/2)$ dominates the tail of the integrand (because $r^{-1} f^{[k]}(1/r)$ has polynomial structure), ensuring the finiteness of the upper bound and therefore of $V(\mathbf{z})$. \square

Proposition B.2 (Elliptical point process representation). *Consider the Poisson process with points $\{R_i \mathbf{W}_{s^*,i}, i = 1, 2, \dots\}$, where $\mathbf{W}_{s^*,i}$ are iid standard Gaussian vectors defined*

over a configuration of sites $\mathbf{s}^* = \{\mathbf{s}_1, \dots, \mathbf{s}_D\}$ with correlation matrix $\Sigma_{\mathbf{s}^*}$, and $\{R_i\}$ are the points of a Poisson process distributed according to one of the intensity measures $\kappa_{\gamma}^{[k]}$ given for $k = 1, 2, 3$ in (15), (16) and (17) respectively, with stochastic independence between $\mathbf{W}_{\mathbf{s}^*,i}$ and $\{R_i\}$. Then the Poisson process has elliptical representation

$$\{R_i \mathbf{W}_{\mathbf{s}^*,i}, i = 1, 2, \dots\} \stackrel{D}{=} \{\tilde{R}_i \Sigma_{\mathbf{s}^*}^{1/2} \mathbf{S}_i, i = 1, 2, \dots\} \quad (33)$$

with a Poisson process $\{\tilde{R}_i, i = 1, 2, \dots\} \stackrel{D}{=} \{R_i R_{\mathbf{W},i}, i = 1, 2, \dots\}$, where $R_{\mathbf{W},i} > 0$ are iid random variables following the χ_D -distribution F_{χ_D} with density

$$f_{\chi_D}(x) = 2^{1-D/2} \Gamma(D/2)^{-1} x^{D-1} \exp(-x^2/2), \quad x > 0,$$

independently of iid random vectors \mathbf{S}_i uniformly distributed over the unit sphere \mathcal{S}_{D-1} . The intensity measure $\tilde{\kappa}_{\gamma}^{[k]}$ of $\{\tilde{R}_i, i = 1, 2, \dots\}$ is characterized through its tail measure

$$\tilde{\kappa}_{\gamma}^{[k]}[z, \infty) = \int_0^{\infty} \kappa_{\gamma}^{[k]}[z/r, \infty) f_{\chi_D}(r) dr = \int_0^{\infty} \bar{F}_{\chi_D}(z/r) f^{[k]}(r) dr, \quad z > 0. \quad (34)$$

Proof. A multivariate standard Gaussian random vector $\mathbf{W}_{\mathbf{s}^*}$ has elliptical representation $\mathbf{W}_{\mathbf{s}^*} \stackrel{D}{=} R_{\mathbf{W}} \Sigma_{\mathbf{s}^*}^{1/2} \mathbf{S}$ where $R_{\mathbf{W}} > 0$ and $R_{\mathbf{W}}^2$ follows a χ_D^2 -distribution, independently of a uniform random vector \mathbf{S} over the unit sphere \mathcal{S}_{D-1} , and with $\Sigma_{\mathbf{s}^*}^{1/2} \Sigma_{\mathbf{s}^*}^{T/2} = \Sigma_{\mathbf{s}^*}$. Therefore, the Poisson process used in the max-id construction is characterized by the elliptical construction (33). The tail measure representations (34) are obtained by integrating out the distribution of the random factors $R_{\mathbf{W},i}$ in the Poisson points $\{R_i R_{\mathbf{W},i}, i = 1, 2, \dots\}$; directly switching between the two representations is possible via an integration-by-parts argument. \square

Proposition B.3 (Weibull tail decay). *Under the assumptions of Proposition B.2, the intensity measures $\tilde{\kappa}_{\gamma}^{[k]}$ in (34) of the radial Poisson process $\{\tilde{R}_i, i = 1, 2, \dots\}$, $k = 1, 2, 3$, have univariate Weibull tail with Weibull coefficient $2\beta/(\beta + 2)$.*

Proof. For ease of notation, we omit the superscript $[k]$ and subscript γ in $\tilde{\kappa}_{\gamma}^{[k]}$ in the following and denote the distribution function of $R_{\mathbf{W}}$ by F_{χ_D} . We write the tail measure of $\tilde{\kappa}$ as follows,

$$\tilde{\kappa}[z, \infty) = \underbrace{\int_0^1 \bar{F}_{\chi_D}(z/r) f^{[k]}(r) dr}_{\tilde{\kappa}_1[z, \infty)} + \underbrace{\int_1^{\infty} \bar{F}_{\chi_D}(z/r) f^{[k]}(r) dr}_{\tilde{\kappa}_2[z, \infty)},$$

where $\tilde{\kappa}_1$ is an infinite-mass intensity measure over $(0, \infty)$ due to the infinite number of Poisson points $R_i \leq 1$, while $\tilde{\kappa}_2$ is a finite-mass intensity measure which corresponds to the

points $R_i > 1$. To prove the Weibull tail behavior of $\tilde{\kappa}$, we first show that $\tilde{\kappa}_2$ is Weibull-tailed with Weibull coefficient $2\beta/(\beta + 2)$, and we then show that the tail of $\tilde{\kappa}_1$ is asymptotically dominated by the one of $\tilde{\kappa}_2$ as z tends to infinity. Notice that $\tilde{\kappa}_1[z, \infty)/\tilde{\kappa}_2[z, \infty) \rightarrow 0$ for $z \rightarrow \infty$ if the Weibull coefficients β_1 and β_2 of $\tilde{\kappa}_1$ and $\tilde{\kappa}_2$ respectively satisfy $\beta_1 > \beta_2$. The intensity measure $\tilde{\kappa}_2$ can be represented as $c\tilde{H}$ with $c = \tilde{\kappa}_2[1, \infty) > 0$ and \tilde{H} a probability distribution. Based on results for the product of Weibull-type random variables (Hashorva and Weng, 2014; Huser et al., 2017), one easily shows that \tilde{H} is Weibull-tailed with coefficient $2\beta/(\beta + 2)$, where 2 is the Weibull coefficient of F_{χ_D} . Therefore, $\tilde{\kappa}_2$ is Weibull-tailed with coefficient $2\beta/(\beta + 2)$. To show that the tail of $\tilde{\kappa}_1$ is lighter such that its contribution can be neglected, we now fix an arbitrary small $0 < \varepsilon_1 < 2$ and a constant $C_1 > 0$ such that $\overline{F}_{\chi_D}(r) \leq C_1\sqrt{2\pi}^{-1} \exp(-r^{2-\varepsilon_1})$ for all $r \leq 1$. Then, one has

$$\begin{aligned} \tilde{\kappa}_1[z, \infty) &\leq C_1 \int_0^1 \exp\{-(z/r)^{2-\varepsilon_1}\} f^{[k]}(r) dr \\ &\stackrel{r \rightarrow 1/r}{=} C_1 \int_1^\infty \exp(-z^{2-\varepsilon_1} r^{2-\varepsilon_1}) f^{[k]}(1/r) r^{-2} dr. \end{aligned}$$

For any parameter values of α and β in the construction of $\tilde{\kappa}_\gamma^{[k]}$ and for $z > z_0 > 0$ with some fixed z_0 , we can fix constants $\varepsilon_2 > 0$ with $\varepsilon_1 + \varepsilon_2 < 2$ and $C_2 > 0$ such that

$$C_1 \exp(-z^{2-\varepsilon_1} r^{2-\varepsilon_1}) f^{[k]}(1/r) r^{-2} \leq C_2 (2 - \varepsilon_1 - \varepsilon_2) \exp(-z^{2-\varepsilon_1} r^{2-\varepsilon_1-\varepsilon_2}) z^{2-\varepsilon_1} r^{1-\varepsilon_1-\varepsilon_2}, \quad r \geq 1,$$

which yields the upper bound

$$\begin{aligned} \tilde{\kappa}_1[z, \infty) &\leq C_2 \int_1^\infty (2 - \varepsilon_1 - \varepsilon_2) \exp(-z^{2-\varepsilon_1} r^{2-\varepsilon_1-\varepsilon_2}) z^{2-\varepsilon_1} r^{1-\varepsilon_1-\varepsilon_2} dr \\ &= -C_2 \exp(-z^{2-\varepsilon_1} r^{2-\varepsilon_1-\varepsilon_2}) \Big|_{r=1}^{r=\infty} = C_2 \exp(-z^{2-\varepsilon_1}). \end{aligned}$$

By choosing ε_1 small enough, we get that $2 - \varepsilon_1 > 2\beta/(\beta + 2)$, so that the Weibull-type tail of $\tilde{\kappa}_2$ dominates $\tilde{\kappa}_1$, and therefore $\tilde{\kappa}$ is Weibull-tailed with Weibull coefficient $2\beta/(\beta + 2)$. \square

A consequence of Proposition B.3 is that the contribution of the points R_i with $R_i \leq 1$ can be neglected in the asymptotic analysis of the tail behavior of a max-id random vector.

Proposition B.4 (Asymptotic independence in bivariate max-id vectors).

Consider the bivariate max-id distribution $\mathbf{Z} = (Z_1, Z_2)^T = \max_{i=1,2,\dots} R_i (W_{1,i}, W_{2,i})^T$, constructed using $(W_{1,i}, W_{2,i})^T$ iid copies of a bivariate standard Gaussian random vector $\mathbf{W} = (W_1, W_2)^T$ with correlation coefficient $\rho \in (-1, 1)$, independent of the points $\{R_i\}$ of a

Poisson process distributed according to one of the intensity measures $\kappa_{\gamma}^{[k]}$, $k = 1, 2, 3$. Then, for $\beta > 0$ (and/or $\alpha > 0$ for $\kappa_{\gamma}^{[1]}$), the distribution of \mathbf{Z} is asymptotically independent with coefficient of tail dependence

$$\eta = \{(1 + \rho)/2\}^{\beta/(\beta+2)}. \quad (35)$$

Proof. Proposition B.2 provides the equivalent elliptical construction of \mathbf{Z} as

$$\mathbf{Z} \stackrel{D}{=} \{\tilde{R}_i \Sigma^{1/2} \mathbf{S}_i, i = 1, 2, \dots\}, \quad \Sigma = \begin{pmatrix} 1 & \rho \\ \rho & 1 \end{pmatrix},$$

with bivariate iid spherical random vectors \mathbf{S}_i . According to Proposition B.3, the Poisson process $\{\tilde{R}_i\}$ is Weibull-tailed with coefficient $2\beta/(2 + \beta)$. Owing to the elliptical structure of the bivariate mean measure Λ and the tail approximation (4), we can apply results on the joint tail behavior of elliptical distributions with Weibull-type radial variables (Hashorva, 2010; Huser et al., 2017) to characterize the joint tail behavior of the bivariate max-id distribution G of \mathbf{Z} , which yields the coefficient coefficient of tail dependence $\eta = \{(1 + \rho)/2\}^{\beta/(\beta+2)}$; see Hashorva (2010, Theorem 2.1 and Example 3) and Huser et al. (2017, Theorem 2). \square

References

Alzaid, A. A. and Proschan, F. (1994) Max-infinite divisibility and multivariate total positivity. *Journal of applied probability* **31**(03), 721–730.

Bevilacqua, M., Gaetan, C., Mateu, J. and Porcu, E. (2012) Estimating Space and Space-Time Covariance Functions for Large Data Sets: A Weighted Composite Likelihood Approach. *Journal of American Statistical Association* **107**(497), 268–280.

Bienvenüe, A. and Robert, C. Y. (2017) Likelihood inference for multivariate extreme value distributions whose spectral vectors have known conditional distributions. *Scandinavian Journal of Statistics* **44**(1), 130–149.

Bortot, P. and Tawn, J. A. (1998) Models for the extremes of Markov chains. *Biometrika* **85**(4), 851–867.

Castruccio, S., Huser, R. and Genton, M. G. (2016) High-order Composite Likelihood Inference for Max-Stable Distributions and Processes. *Journal of Computational and Graphical Statistics* **25**(4), 1212–1229.

Davison, A. C. and Gholamrezaee, M. M. (2012) Geostatistics of extremes. *Proceedings of the Royal Society A: Mathematical, Physical & Engineering Sciences* **468**(2138), 581–608.

Davison, A. C. and Huser, R. (2015) Statistics of Extremes. *Annual Review of Statistics and its Application* **2**, 203–235.

Davison, A. C., Padoan, S. and Ribatet, M. (2012) Statistical Modelling of Spatial Extremes (with Discussion). *Statistical Science* **27**(2), 161–186.

Dombry, C. and Eyi-Minko, F. (2013) Regular conditional distributions of continuous max-infinitely divisible random fields. *Electronic Journal of Probability* **18**(7), 1–21.

Dombry, C., Genton, M. G., Huser, R. and Ribatet, M. (2016) Full likelihood inference for max-stable data. Submitted.

Esary, J. D., Proschan, F. and Walkup, D. W. (1967) Association of random variables, with applications. *The Annals of Mathematical Statistics* **38**(5), 1466–1474.

Giné, E., Hahn, M. G. and Vatan, P. (1990) Max-infinitely divisible and max-stable sample continuous processes. *Probability theory and related fields* **87**(2), 139–165.

de Haan, L. (1984) A Spectral Representation for Max-stable Processes. *Annals of Probability* **12**(4), 1194–1204.

Hashorva, E. (2010) On the residual dependence index of elliptical distributions. *Statistics & Probability Letters* **80**(13), 1070–1078.

Hashorva, E. and Weng, Z. (2014) Tail asymptotic of Weibull-type risks. *Statistics* **48**, 1155–1165.

Huser, R. and Davison, A. C. (2013) Composite likelihood estimation for the Brown–Resnick process. *Biometrika* **100**(2), 511–518.

Huser, R., Davison, A. C. and Genton, M. G. (2016) Likelihood estimators for multivariate extremes. *Extremes* **19**(1), 79–103.

Huser, R., Opitz, T. and Thibaud, E. (2017) Bridging Asymptotic Independence and Dependence in Spatial Extremes Using Gaussian Scale Mixtures. *Spatial Statistics* To appear.

Huser, R. and Wadsworth, J. L. (2017) Modeling spatial processes with unknown extremal dependence class. *arXiv:1703.06031*.

Kaufmann, E. (2000) Penultimate approximations in extreme value theory. *Extremes* **3**(1), 39–55.

Kojadinovic, I., Segers, J. and Yan, J. (2011) Large-sample tests of extreme-value dependence for multivariate copulas. *Canadian Journal of Statistics* **39**(4), 703–720.

Ledford, A. W. and Tawn, J. A. (1996) Statistics for near independence in multivariate extreme values. *Biometrika* **83**(1), 169–187.

Opitz, T. (2013) Extremal t processes: Elliptical domain of attraction and a spectral representation. *Journal of Multivariate Analysis* **122**, 409–413.

Opitz, T. (2016) Modeling asymptotically independent spatial extremes based on Laplace random fields. *Spatial Statistics* **16**, 1–18.

Padoan, S. A. (2013) Extreme dependence models based on event magnitude. *Journal of Multivariate Analysis* **122**, 1–19.

Padoan, S. A., Ribatet, M. and Sisson, S. A. (2010) Likelihood-Based Inference for Max-Stable Processes. *Journal of the American Statistical Association* **105**(489), 263–277.

Papastathopoulos, I. and Tawn, J. A. (2013) Extended generalised Pareto models for tail estimation. *Journal of Statistical Planning and Inference* **143**(1), 131–143.

Resnick, S. I. (1987) *Extreme values, regular variation and point processes*. Springer.

Schlather, M. (2002) Models for Stationary Max-Stable Random Fields. *Extremes* **5**(1), 33–44.

Simpson, D. P., Rue, H., Martins, T. G., Riebler, A. and Sørbye, S. H. (2017) Penalising model component complexity: A principled, practical approach to constructing priors. *Statistical Science* **32**(1), 1–28.

Stephenson, A. and Tawn, J. (2005) Exploiting occurrence times in likelihood inference for componentwise maxima. *Biometrika* **92**(1), 213–227.

Stephenson, A. G., Lehmann, E. A. and Phatak, A. (2016) A max-stable process model for rainfall extremes at different accumulation durations. *Weather and Climate Extremes* **13**, 44–53.

Thibaud, E., Aalto, J., Cooley, D. S., Davison, A. C. and Heikkinen, J. (2016) Bayesian inference for the Brown–Resnick process, with an application to extreme low temperatures. *Annals of Applied Statistics* **10**(4), 2303–2324.

Thibaud, E. and Opitz, T. (2015) Efficient inference and simulation for elliptical Pareto processes. *Biometrika* **102**(4), 855–870.

Tukey, J. W. (1961) Discussion, emphasizing the connection between analysis of variance and spectrum analysis. Technical report, Princeton University, Department of Mathematics, Princeton, N.J.

Varin, C., Reid, N. and Firth, D. (2011) An overview of composite likelihood methods. *Statistica Sinica* **21**(2011), 5–42.

Wadsworth, J. L. (2015) On the occurrence times of componentwise maxima and bias in likelihood inference for multivariate max-stable distributions. *Biometrika* **102**(3), 705–711.

Wadsworth, J. L. and Tawn, J. A. (2012) Dependence modelling for spatial extremes. *Biometrika* **99**(2), 253–272.

Westra, S. and Sisson, S. A. (2011) Detection of non-stationarity in precipitation extremes using a max-stable process model. *Journal of Hydrology* **406**(1–2), 119–128.